Atmospheric
Chemistry
and Physics

Hygroscopicity of isoprene-derived secondary organic aerosol mixture proxies: importance of diffusion and salting-in effects

Nahin Ferdousi-Rokib[1,a]**, N. Cazimir Armstrong**[2]**, Stephanie Jacoby**[3]**, Alana J. Dodero**[4]**, Martin Changman Ahn**[1]**, Ergine Zephira Remy**[1]**, Zhenfa Zhang**[2]**, Avram Gold**[2]**, Joseph L. Woo**[5]**, Yue Zhang**[4]**, Jason D. Surratt**[2,6]**, and Akua A. Asa-Awuku**[1,3]

[1]Department of Chemical and Biomolecular Engineering, University of Maryland,
College Park, MD 20742, United States
[2]Department of Environmental Sciences and Engineering, University of North Carolina at Chapel Hill,
Chapel Hill, North Carolina 27599, United States
[3]Department of Chemistry and Biochemistry, University of Maryland, College Park, MD 20742, United States
[4]Department of Atmospheric Sciences, Texas A&M University, College Station, Texas 77843, United States
[5]Department of Chemical and Biomolecular Engineering, Lafayette College, Easton, PA 18042, United States
[6]Department of Chemistry, University of North Carolina at Chapel Hill, Chapel Hill,
North Carolina 27599, United States
[a]now at: Department of Environmental Health and Engineering, Whiting School of Engineering,
Johns Hopkins University, Baltimore, MD 21218, United States

Correspondence: Nahin Ferdousi-Rokib (ferdousn19@gmail.com) and Akua A. Asa-Awuku
(asaawuku@umd.edu)

Abstract. Isoprene-derived secondary organic aerosol (SOA) constituents, such as the 2-methyltetrols (2-MT) and 2-methyltetrol sulfates (2-MTS), have been readily detected in atmospheric aerosols (PM$_{2.5}$) and within mixtures containing ammonium sulfate (AS). Despite its prevalence, the water uptake of 2-MT, 2-MTS, and their mixtures is not well understood. In this study, we determine the physicochemical properties (e.g., surface activity, diffusivity, phase morphology) of synthesized 2-MT and 2-MTS samples and their mixtures with AS. 2-MT and 2-MTS have been identified as surface active and viscous. Thus, dynamic surface tension ($\sigma_{s/a}$) measurements were taken to determine organic diffusion coefficients (D_s). The droplet growth of organic / AS mixtures was measured under subsaturated conditions using a humidified tandem differential mobility analyzer (H-TDMA) at 88.2 % RH ±1.5 %. Droplet activation was measured under supersaturated (> 100 % RH) conditions using a cloud condensation nuclei counter (CCNC); supersaturation (SS) ranged from 0.3 %–1.4 %. Hygroscopicity in both regimes was parameterized by the single hygroscopicity parameter κ.

This study demonstrates how diffusion and salting-in effects influence the water uptake of synthesized, isoprene-derived SOA mixtures. Results show that when mixed with AS, organic diffusion for 2-MTS / AS becomes an order of magnitude faster, while 2-MT diffusivity remains unchanged. Both 2-MT / AS and 2-MTS aerosols present a plateau in subsaturated κ values close to pure AS. However, under supersaturated conditions, 2-MTS / AS behaves ideally and well mixed and can be characterized by κ-Köhler theory. Isoprene-derived SOAs like 2-MT and 2-MTS samples are ubiquitous, and thus, the impact from biogenic sources and its non-ideal thermodynamic properties must be considered in aerosol–cloud interactions.

1 Introduction

Fine aerosol particles ($PM_{2.5}$) suspended within our atmosphere are a major contributor to Earth's radiative forcing and uncertainties in global temperature projections (Intergovernmental Panel on Climate, 2023). Aerosol–cloud radiative forcing uncertainty is attributed to aerosols' ability to form and modify cloud properties, known as aerosol–cloud interactions or the "aerosol indirect effect" (Köhler, 1936; Twomey, 1959; Twomey, 1974; Albrecht, 1989; Intergovernmental Panel on Climate, 2023). An aerosol's ability to alter droplet formation is dependent on its hygroscopicity or water uptake behavior under supersaturated conditions (RH > 100 %). In the presence of water vapor, aerosols present a surface for condensation; droplet activation depends on aerosol particle chemical composition and size (Seinfeld and Pandis, 1998; Petters and Kreidenweis, 2007). The aerosol droplets can reach a point of unstable and uncontrollable growth, thereby acting as cloud condensation nuclei (CCN) (Köhler, 1936; Seinfeld and Pandis, 1998).

Droplet models can apply Köhler theory to estimate aerosol droplet growth and CCN activity (Köhler, 1936). In traditional Köhler theory, it is assumed that all aerosol solutes instantaneously dissolve and contribute to water uptake (Petters and Kreidenweis, 2007). Aerosol hygroscopicity is thus parameterized by Köhler theory through the single hygroscopicity parameter κ; κ of mixed composition is often estimated by the Zdanovskii–Stokes–Robinson (ZSR) mixing rule and it is assumed that an individual solute's contribution to hygroscopicity is scaled by its volume fraction (Petters and Kreidenweis, 2007). Thus, knowing aerosol composition is critical for understanding CCN formation. However, κ-Köhler predictions of aerosol CCN activity neglect solute physicochemical properties that may alter droplet growth. Previous studies have shown that droplet-altering properties may be present within aerosols, such as the presence of complex morphologies (e.g., inner core–outer layer), surface activity, or salting-in/salting-out effects; as a result, discrepancies between experimentally determined κ and κ-Köhler predictions may occur (Asa-Awuku and Nenes, 2007; Bertram et al., 2011; Song et al., 2013; Prisle, 2021; Riemer et al., 2019; Ott et al., 2020; Malek et al., 2023).

Field studies have observed the presence of internally mixed aerosols containing both inorganic and organic compounds (Saxena, 1995; Murphy et al., 1998; Pratt and Prather, 2010). Inorganic aerosols, primarily composed of salts like ammonium sulfate (AS) and sodium chloride, have well-defined hygroscopic properties. The ionic behavior of inorganic compounds promotes instantaneous dissolution in water and contributes to CCN activation (Cziczo et al., 1997; Seinfeld, 2003; Rose et al., 2008; Laskina et al., 2015). However, fine organic aerosols (OAs) pose a greater challenge to aerosol hygroscopicity predictions. OAs constitute 20 %–50 % of atmospheric fine aerosol mass and are diverse in composition. OAs can be directly emitted into the atmosphere, referred to as primary organic aerosols (POAs) (Kanakidou et al., 2005). POAs can originate from anthropogenic (e.g., biomass burning and coal combustion) and biogenic (e.g., pollen) sources (Seinfeld and Pandis, 1998; Kanakidou et al., 2005). In addition to POA, secondary organic aerosol (SOA) can be formed through multigeneration gas-phase oxidation reactions of volatile organic compounds (VOCs) or multiphase reactions of semi-volatile/low-volatility organic compounds (SVOCs/LVOCs) (Kanakidou et al., 2005). SOA is ubiquitous in the atmosphere, forming a major component of fine OA mass (Zhang et al., 2007; Srivastava et al., 2022). For example, a study by Zhang et al. (2007) found that SOA contributed 65 % to 95 % of OA mass in urban and remote regions. Furthermore, SOAs have been readily detected in mixtures with inorganic components, such as AS (Yang et al., 2009; Zhu et al., 2017); indeed, a study by Zhu et al. (2017) estimated 66 % of SOA as being internally mixed with sulfate. Thus, in addition to understanding pure organic compounds, it is important to also study organic–inorganic interactions.

Previous studies have determined that a significant contributor to SOA is the aqueous-phase chemical processing of isoprene-derived oxidation products (Claeys et al., 2004; Kanakidou et al., 2005). Isoprene is a VOC emitted from biogenic sources and is considered one of the most abundant biogenic VOCs (BVOCs). Isoprene emissions have been estimated to be $\sim 500\,\mathrm{Tg\,C\,yr^{-1}}$, rivaling methane emissions (Guenther et al., 2012; Sindelarova et al., 2014). Under alkyl peroxy radical ($RO_2^\bullet$) + hydroperoxy radical ($HO_2^\bullet$) dominant conditions, isoprene is photochemically oxidized by gas-phase hydroxyl radicals ($^\bullet OH$) to form large quantities of isoprene-derived epoxydiols (IEPOX) (Paulot et al., 2009). IEPOX is then able to partition into acidic-sulfate-containing aerosol particles to produce isoprene-derived SOA (Surratt et al., 2010; Lin et al., 2012; Gaston et al., 2014; Riva et al., 2019), which consists largely of 2-methyltetrols (2-MT) and 2-methyltetrol sulfates (2-MTS).

Both 2-MT and 2-MTS were previously detected in atmospheric $PM_{2.5}$. For example, a study by Claeys et al. (2004) found that 2-MT contributed 2 % of organic carbon detected in $PM_{2.5}$ collected from the Amazon rainforest. Additional field studies have also found that 2-MTS can contribute 0.3 %–16.5 % of total organic carbon in both the Amazon rainforest and Southeast US (Chan et al., 2010; Froyd et al., 2010; Hettiyadura et al., 2019; Riva et al., 2019; Chen et al., 2021; Hughes et al., 2021). The formation of both compounds can also alter aerosol particle composition and phase state (Zhang et al., 2019a, b). For example, 2-MT and 2-MTS have been observed to be in a semisolid or glassy state in aerosol particles (Chen et al., 2023). Highly viscous SOA can exist in a glassy state; SOA viscosities can range from 10^2 to $10^{12}\,\mathrm{Pa\,s}$ for ultraviscous liquids or $> 10^{12}\,\mathrm{Pa\,s}$ for amorphous, extremely viscous compounds (Virtanen et al., 2010; Renbaum-Wolff et al., 2013; Zhang et al., 2015). Viscosity can influence organic solute dissolution in droplets

by slowing diffusion through the aqueous phase (Renbaum-Wolff et al., 2013). As a result, slower organic diffusion rates can influence gas partitioning, particle shape, chemical aging, multiphase reactions, and aerosol droplet growth (Riipinen et al., 2011; Shiraiwa and Seinfeld, 2012; Zhang et al., 2015). Furthermore, studies incorporating SOA viscosity and phase state into larger, global-scale models have observed changes to CCN and ice nuclei (IN) formation predictions (Riipinen et al., 2011; Shiraiwa et al., 2017; Wolf et al., 2021). Thus, probing the viscosity and resulting diffusion limitations may be necessary for understanding 2-MT and 2-MTS water uptake properties (Chen et al., 2023).

Similar to other complex organic mixtures, the water uptake ability of isoprene-derived SOA can be further complicated when mixed with inorganic components, such as AS. Previous studies have observed the presence of internally mixed SOA/AS aerosols in both the southeast US and Amazon; in both regions a strong presence of 2-MT and 2-MTS has been observed (Chan et al., 2010; Froyd et al., 2010; Bondy et al., 2018; Riva et al., 2019; Wu et al., 2019). The presence of inorganic salts in aerosol mixtures can influence phase state based on organic physicochemical properties (Topping, 2010; Ruehl et al., 2012; Ruehl et al., 2016; Malek et al., 2023). Inorganic compounds can result in water-solubility-limited and/or surface-active organics partitioning to a separated phase (Ruehl et al., 2012, 2016; Freedman, 2017; Kang et al., 2020). As a result, the partitioned aerosols can exhibit a phase-separated morphology (Ruehl et al., 2012, 2016; Freedman, 2017; Kang et al., 2020; Malek et al., 2023). However, inorganic salts may also enhance organic dissolution, known as "salting in" (Riva et al., 2019). For instance, studies have observed increased diffusion in viscous SOA particles through the aqueous droplet phase in the presence of inorganic salts (Reid et al., 2018; Jeong et al., 2022; Sheldon et al., 2023). Increased diffusion is a result of salts disrupting the hydrogen bonding network between neighboring organic molecules (Reid et al., 2018; Jeong et al., 2022; Sheldon et al., 2023). Therefore, organic physicochemical properties (surface activity, viscosity) of SOA, such as 2-MT and 2-MTS, must be better defined to better predict mixed SOA/AS aerosol CCN activity. To our knowledge there are no studies to date that investigate 2-MT and 2-MTS aerosol water uptake, water uptake of mixtures with AS, and the potential effect of physicochemical properties on CCN activity predictions.

In this study, we investigated the surface activity, diffusivity, droplet growth, and water uptake of 2-MT, 2-MTS, and their mixtures with AS. 2-MT and 2-MTS surface tension values were experimentally determined. A previous study by Ekström et al. (2009) found 2-MT to be moderately surface active. However, the surface activity of 2-MTS has not been characterized, and potential organic surface tension depression in the presence of AS has not been explored for both organics. In tandem with surface tension measurements, this study estimated diffusion coefficients of

both compounds to explore the effects of viscosity and diffusivity on aerosol water uptake. Aerosol κ-hygroscopicity values for pure organic and organic / AS mixtures were experimentally determined under both subsaturated conditions ($< 100\,\%\,RH$) and supersaturated ($> 100\,\%\,RH$) conditions to observe both droplet growth and CCN activity, respectively. κ-hygroscopicity measurements were then compared to κ-Köhler hygroscopicity theory to evaluate the efficacy of traditional full dissolution and negligible viscosity assumptions in predicting the CCN activity of both compounds and their mixtures. Lastly, atomic force microscopy (AFM) measurements on mixed particles were conducted to further understand particle morphology. The following work provides a comprehensive analysis of the wide range of physicochemical properties that may influence the droplet growth of 2-MT and 2-MTS mixed with AS.

2 Experimental methods

2.1 Experimental chemicals

For this study, ammonium sulfate (AS, $(NH_4)_2SO_4$; Thermo Fisher Scientific, $> 99.0\,\%$), was purchased and used without further purification. 2-methyltetrol (2-MT) and 2-methyltetrol sulfate (2-MTS) samples were synthesized using the published procedure of Cui et al. (2018). 2-MT was determined to be $> 98\,\%$ pure. The purity of 2-MTS was determined to be $\sim 73\,wt\,\%$, with remaining sample mass estimated to be $3\,wt\,\%$ AS and $24\,wt\,\%$ sodium methyl sulfate (SMS). It should be noted that from here on, the 2-MTS sample refers to a prescribed synthesized mixture, and subsequent calculations account for the estimated contributions of AS and SMS.

2.2 Surface tension measurements

The surface tension of 2-MT, 2-MTS, and their mixtures with AS was measured at atmospherically relevant aqueous-phase concentrations. Due to the limited amounts of synthesized sample, mixed amounts were judiciously selected to mimic mixture ratios previously reported in the literature. Specifically, a study by Cope et al. (2021) found that 2-MT concentrations in the atmosphere reached an upper bound of $300\,mM$. Therefore, stock solutions of $300\,mM$ 2-MT and 2-MTS were prepared using deionized (DI) water. Furthermore, it is assumed that surface tension measurements at dilutions higher than $300\,mM$ are also relevant for droplet growth. A study by Bain et al. (2023) found that aerosol surface tension can be approximated from surface tension measurements of bulk mixtures composed of $< 100\,mM$ organic component. Additionally, recent studies (Mikhailov et al., 2024; Ferdousi-Rokib et al., 2025) also support the application of more dilute concentration regimes to predict droplet growth. A recent study by Mikhailov et al. (2024) found that surface tension depression observed in

bulk dilute surface tension measurements was reflective of aerosol properties. Ferdousi-Rokib et al. (2025) also found that salting-out effects can be approximated in mixtures having < 100 mM organic component. Thus, in this work, the stock solutions were diluted to a 3–94 mM range; each stock solution and subsequent dilution concentrations are provided in Tables S1–S5 in the Supplement.

Droplet surface tension ($\sigma_{s/a}$) was measured using a pendant drop tensiometer with a modified profile analysis tensiometer (SINTERFACE Inc.); the experimental setup has been described in Fertil et al. (2025). Briefly, the pendant drop tensiometer generates a droplet of solution ($< 10\,\mu$L) suspended from a 0.9 mm diameter needle (Beier et al., 2019; Fertil et al., 2025). Droplets remain suspended for 300 s to reach equilibrium; at each time step (~ 1 s), the droplet $\sigma_{s/a}$ was obtained from fitting the droplet curvature to the Young–Laplace Equation (Fordham and Freeth, 1948; Spelt, 1996; Padró et al., 2010). Surface tension measurements were run in triplicate; prior to each measurement, the tensiometer was flushed with DI water and ~ 2 mL of solution. Measurements were obtained at ambient room conditions, with a temperature range of 20.2–22 °C and relative humidity range of 40 %–45 % RH.

As the droplet equilibrates, surface tension changes, which is attributed to the accumulation of solute diffusing to the droplet surface (Joos and Rillaerts, 1981; Eastoe et al., 1998; Chernyshev and Skliar, 2015). As the solute saturates the surface, surface tension reaches equilibrium (Ross, 1945). The accumulation of solute at the surface and resulting concentration gradient within the droplet can be described by Fick's second law:

$$\frac{\partial C}{\partial t} = D_s \frac{\partial^2 C}{\partial x^2}, \tag{1}$$

where concentration over time $\frac{\partial C}{\partial t}$ is proportional to the second derivative concentration over position $\frac{\partial^2 C}{\partial x^2}$ and the diffusion coefficient D_s (m² s⁻¹). The dynamic surface tension can be correlated with solute diffusion over time as (Joos and Rillaerts, 1981)

$$\sigma_t = \sigma_0 - 2RTC\left(\frac{D_s t}{\pi}\right)^{0.5}, \tag{2}$$

where σ_0 is the starting surface tension, σ_t is the surface tension at specified time t, R is the universal gas constant, T is temperature, and C is organic molar concentration. Here, evaporation effects are negligible during the short suspension times. Therefore, the organic molar concentration C is equivalent to the droplet solution concentration as Eq. (2) can then be rearranged to solve for D_s using dynamic surface tension measurements.

2.3   Aerosol experimental methods

2.3.1   Aerosol generation

Solutions of 0.1 g L⁻¹ total solute (2-MT, 2-MTS, and mixtures with AS) were prepared using ultra-purified Millipore water (18 MΩ cm). Mixtures compositions are provided in Table S6. Polydisperse aerosols were then generated by passing each aqueous solution through a constant-output Collison Nebulizer (Atomizer, TSI 3076); the generated aerosols were then dried to < 5 % RH using two silica gel dyers in series. Aerosols were then analyzed for their water uptake properties under sub- and supersaturated conditions. To determine aerosol phase morphology, atomic force microscopy (AFM) images were also obtained. In addition to water uptake and AFM measurements, organic density and shape factor were measured; for details on density and shape factor measurements, see Armstrong et al. (2025).

2.3.2   Water uptake measurements

A humidified tandem differential mobility analyzer (H-TDMA) measured droplet growth under subsaturated conditions. Dry, polydisperse aerosols were size-selected at 100, 150, and 200 nm by an electrostatic classifier (DMA 1, TSI 3082; flow rate $= 0.3$ L min⁻¹) and humidified using a Nafion humidification line (PermaPure M.H. series); particles were humidified at 88.2 ± 1.5 % RH. Selected dry diameters are often assumed to be spherical, thus having a shape factor (χ) of 1 (DeCarlo et al., 2004). Aerodynamic aerosol classifier (AAC) shape factor measurements confirmed 2-MT and 2-MTS sphericity (Armstrong et al., 2025). The wet diameter (D_w) was measured using a second electrostatic classifier (DMA 2, TSI 3082; flow rate $= 0.3$ L min⁻¹); the ratio of D_w to the dry-size-selected diameter (D_d) is equal to the growth factor (G_F). The experimental setup is provided in Fig. S1 in the Supplement. To calibrate the H-TDMA, a 0.1 g L⁻¹ solution of AS was aerosolized; dried AS aerosols were size-selected at 100 and 150 nm. Dried AS aerosol G_F and instrument RH were measured, with calibration measurements repeated multiple times as reported in Table S7. The experimental solutions were then aerosolized, and G_F was obtained for each solution; G_F is used to calculate the hygroscopicity parameter under subsaturated conditions, $\kappa_{\text{H-TDMA}}$. In addition to subsaturated conditions, water uptake was measured under supersaturated (SS) conditions using a CCNC-100 (Droplet Measurement Technologies); the experimental setup is provided in Fig. S2. The theory and operation of the CCNC have been previously described (Roberts and Nenes, 2005; Lance et al., 2006; Rose et al., 2008). The Scanning Mobility CCN Analysis (SMCA) protocol was used to measure droplet activation (Moore et al., 2010). Briefly, the dried polydisperse aerosols were passed through an electrostatic classifier (TSI 3080) in scanning mode and charged; scanning mode operated from 8–352 nm for 135 s. The DMA operated at a sheath-to-aerosol

flow rate ratio of $10:1$ and aerosol sample flow rate of $0.8\,\mathrm{L\,min^{-1}}$. The monodisperse, size-selected aerosol stream was then sampled by a condensation particle counter (CPC, TSI 3776, flow rate $= 0.3\,\mathrm{L\,min^{-1}}$) and the CCNC-100 (flow rate $= 0.5\,\mathrm{L\,min^{-1}}$) in parallel. The CPC counted the number concentration of dry particles at a given particle size (condensation nuclei, N_{CN}). The CCNC exposed the particles to $0.3\,\%$–$1.4\,\%$ SS, and the number concentration of particles activated (N_{CCN}) was measured. The instrument setup was calibrated using AS (Rose et al., 2008), and the calibration data are provided in Table S8 and Fig. S3.

The CPC counted the number concentration of dry particles at a given particle size (condensation nuclei, N_{CN}). The CCNC exposed the particles to $0.3\,\%$–$1.4\,\%$ SS and the number concentration of particles activated (N_{CCN}) were measured. The instrument setup was calibrated using AS (Rose et al., 2008) and the calibration data are provided in Table S8 and Fig. S3.

CCN data of AS and experimental solutions were analyzed using the Python-based CCN Analysis Toolkit (PyCAT 1.0) (Gohil, 2022; Gohil and Asa-Awuku, 2022). PyCAT is a Python version of SMCA and is available on GitHub for public use. The analysis toolkit calculated the activation ratio $N_{\mathrm{CCN}}/N_{\mathrm{CN}}$ for each dry particle size. The activation ratios were fitted using a sigmoid curve and the critical diameter ($D_{\mathrm{p},\,50}$) was found, at which $\sim 50\,\%$ of the dry particles activate. A charge correction is applied in PyCAT using the multi-charge correction algorithm previously described (Fuchs, 1963; Wiedensohler, 1988). The obtained critical diameter of each solution is then used to calculate the single hygroscopicity parameter under supersaturated conditions, κ_{CCN}.

2.3.3 Atomic force microscopy (AFM) morphology

Atomic force microscopy (AFM) measurements were utilized to characterize aerosol phase morphology. 2-MTS, 2-MTS / AS, and 2-MT / AS particles were collected onto silicon substrates (Silson Ltd) using a cascade impactor (Sioutas Cascade Impactor, flow rate $= 9\,\mathrm{L\,min^{-1}}$) and stored at room temperature and relative humidity ($40\,\%$–$50\,\%$ RH) prior to analysis. Imaging followed the procedure of Zhang et al. (2018). Briefly, particles were imaged in a $5 \times 5\,\mu\mathrm{m}$ region using a Dimension ICON® AFM (Bruker) in tapping mode with resonant frequency of $150\,\mathrm{kHz}$ and spring constant of $5.4\,\mathrm{N\,m^{-1}}$.

2.3.4 Viscosity and diffusion calculation

The viscosity and the diffusion coefficients of the 2-MT and 2-MTS aerosols were calculated using a modified Vogel–Tammann–Fulcher (VTF) equation (DeRieux et al., 2018). The dry glass transition temperature values were determined to be 226 and 276 K from a previous study by Zhang et al. (2019b). The Gordon–Taylor coefficient and the fragility

coefficient were assigned values of 2.5 and 20, respectively. The hygroscopicity values were used from the measurement of H-TDMA of this study.

3 Traditional κ-Köhler theory

Traditionally, water uptake of aerosol particles has been calculated using κ-Köhler theory (Köhler, 1936; Petters and Kreidenweis, 2007). Köhler theory considers aerosol physicochemical properties (e.g., solute density, molecular weight) to describe the equilibrium water vapor saturation ratio at a droplet's surface (S_{eq}). The equilibrium relationship encompasses two competing effects. The Kelvin effect describes the increase in water vapor saturation as a result of the curvature of the droplet; the Kelvin effect is represented by droplet surface tension $\sigma_{\mathrm{s/a}}$. The Raoult (solute) effect competes by decreasing vapor pressure due to the presence of solute in the aqueous droplet; the solute effect is represented by the water activity term, a_{w} (Seinfeld and Pandis, 1998; Wex et al., 2008). For compounds dissolved in water, water activity can be parameterized by the single hygroscopicity parameter, κ, as follows (Petters and Kreidenweis, 2007; Sullivan et al., 2009):

$$\frac{1}{a_{\mathrm{w}}} = 1 + \kappa \frac{V_{\mathrm{s}}}{V_{\mathrm{w}}}, \tag{3}$$

where V_{w} and V_{s} are the volume of water and dry solute, respectively. Therefore, the equilibrium saturation ratio (S_{eq}) over the droplet is described as

$$S_{\mathrm{eq}} = \left(1 + \kappa \frac{D_{\mathrm{d}}^3}{D_{\mathrm{w}}^3 - D_{\mathrm{d}}^3}\right)^{-1} \exp\left(\frac{4\sigma_{\mathrm{s/a}} M_{\mathrm{w}}}{RT\rho_{\mathrm{w}} D_{\mathrm{w}}}\right), \tag{4}$$

where ρ_{w} is the density of water, M_{w} is the molecular weight of water, R is the universal gas constant, and T is the temperature.

κ describes the ability of an aerosol to uptake water assuming full dissolution and can be calculated from the intrinsic properties of the solute as κ_{int} (Sullivan et al., 2009):

$$\kappa_{\mathrm{int}} = \frac{\nu_{\mathrm{s}}\rho_{\mathrm{s}} M_{\mathrm{w}}}{\rho_{\mathrm{w}} M_{\mathrm{s}}} \tag{5}$$

where M_{s} is the molecular weight of solute, ν_{s} is the van't Hoff factor, and ρ_{s} is the density of the solute; Armstrong et al. (2025) found 2-MT and 2-MTS density to be 1.4 and $2.46\,\mathrm{g\,cm^{-3}}$, respectively. To estimate κ-hygroscopicity of aerosols containing more than one compound, the Zdanovskii–Stokes–and Robinson (ZSR) mixing rule can be applied (Petters and Kreidenweis, 2007):

$$\kappa_{\mathrm{ZSR}} = \sum_i \varepsilon_i \kappa_i, \tag{6}$$

where ε_i is the volume fraction of the individual solute component, i.

Experimental data can be used to derive aerosol κ. Under subsaturated ($< 100\%$ RH) conditions, G_F is related to hygroscopicity as follows (Kreidenweis and Asa-Awuku, 2014):

$$\kappa_{\text{H–TDMA}} = \frac{\left(G_F^3 - 1\right)}{\frac{\text{RH}}{\exp\left(\frac{4\sigma_{s/a}M_w}{RT\rho_w D_d G_F}\right)}} - G_F^3 + 1, \tag{7}$$

where $\kappa_{\text{H-TDMA}}$ is subsaturated hygroscopicity, and RH is the relative humidity of the H-TDMA instrument as a decimal. Similarly, for supersaturated ($> 100\%$ RH), the critical diameter correlates to κ as follows (Petters and Kreidenweis, 2007):

$$\kappa_{\text{CCN}} = \frac{4\left(\frac{4\sigma_{s/a}M_w}{RT\rho_w}\right)^3}{27D_{p,50}^3 \ln^2 \text{SS}}, \tag{8}$$

where κ_{CCN} is supersaturated hygroscopicity. It is assumed that droplet surface tension $\sigma_{s/a}$ is equivalent to that of the surface tension of water $\sim 72\,\text{mN m}^{-1}$. Köhler theory also assumes that all solutes are well mixed within the aqueous phase. The Köhler/ZSR model does not account for potential viscosity and diffusivity limitations due to inorganic–organic mixing in the aqueous phase. Therefore, in this study, κ-Köhler values are predicted assuming both 2-MT and 2-MTS are well mixed within the aqueous phase and fully contribute to droplet growth. The applicability of these assumptions is discussed in the later sections. Additionally, a list of variable abbreviations is provided in Table S9.

4 Results

4.1 Surface tension and diffusion

4.1.1 Organic samples

Dynamic pendant drop tensiometer measurements were taken for 2-MT and 2-MTS samples; measurements were performed by hanging droplets $< 10\,\mu\text{L}$ over a period of 300 s. The droplet curvature was measured every 1 s. Average surface tension values were obtained for 2-MT and 2-MTS when droplet surface tension values remained constant (at equilibrium) and are listed in Table S10 and shown in Fig. 1.

In the dilute bulk measurement regime, 2-MT sample (Fig. 1, orange squares) and 2-MTS sample (Fig. 1, purple closed circles) $\sigma_{s/a}$ values are close to pure water ($\sim 72\,\text{mN m}^{-1}$, Fig. 1, blue dashed line). For solutions $< 53\,\text{mM}$ organic concentration, 2-MT and 2-MTS samples exhibit little to no surface activity. Surface activity is similar to the dilute surface tension of pure AS, a non-surface-active compound, which remains $\sim 72\,\text{mN m}^{-1}$ (Fig. 1, red circles, Pruppacher and Klett, 1997). However, for organic solutions $> 53\,\text{mM}$, minimal surface tension depression is observed with $\sigma_{s/a}$ values between ~ 68–$70\,\text{mN m}^{-1}$ (Fig. 1 and Table S10); in comparison, AS surface tension increases with
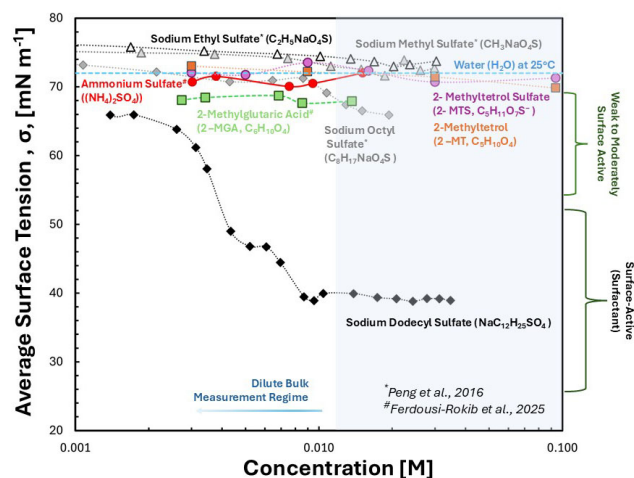

Figure 1. Experimental average surface tension $\sigma_{s/a}$ values of compounds as a function of concentration. Average equilibrium surface tension of synthesized 2-MT ($> 98\,\text{wt}\%$ purity) and 2-MTS ($\sim 73\,\text{wt}\%$ purity) samples are shown as closed orange squares and closed purple circles, respectively. The surface tension of the organosulfates, including sodium ethyl sulfate (black open triangles), sodium methyl sulfate (grey closed triangles), and sodium octyl sulfate (grey closed diamonds) were obtained by Peng et al. (2021). 2-methylglutaric acid (green closed squares) and ammonium sulfate (red closed circles) $\sigma_{s/a}$ were obtained from Ferdousi-Rokib et al. (2025). Sodium dodecyl sulfate (SDS) $\sigma_{s/a}$ is shown as black diamonds. Pure water $\sigma_{s/a}$ at $25\,°\text{C}$ ($\sim 72\,\text{mN m}^{-1}$) is represented as a dashed blue line. Compounds can be categorized as weak to moderately surface active (65–$65\,\text{mN m}^{-1}$) or surface active (surfactants, $< 65\,\text{mN m}^{-1}$) for compounds that can depress surface tension below that of pure water. Bain et al. (2023) consider the dilute bulk measurement regime to be less than $100\,\text{mM}$.

concentration, as observed in Fig. 1 and with previous studies (Pruppacher and Klett, 1997; Hyvärinen et al., 2005; Mikhailov et al., 2024). Therefore, both synthesized 2-MT and 2-MTS sample mixtures can be classified as weakly surface active. A previous study by Riva et al. (2019) observed greater surface tension depression for IEPOX SOA / sulfate mixtures. In particular, enhanced surface tension depression was attributed to organic partitioning and formation of 2-MT and 2-MTS oligomers (Riva et al., 2019).

In comparison to the surface tension of other short-chained particulate organosulfates, such as sodium ethyl sulfate (Fig. 1, black triangles) and sodium methyl sulfate (Fig. 1, grey triangles), 2-MT and 2-MTS have lower dilute surface values (Peng et al., 2021). However, similar to other surface-active organosulfates (sodium ethyl sulfate and sodium octyl sulfate), neither 2-MT sample nor 2-MTS sample surface tension significantly depresses aerosol surface tension (Tables S11 and S14). For example, Mikhailov et al. (2024) observed surface tension depression as low as $\sim 56\,\text{mN m}^{-1}$ for dilute D-glucose / AS mixtures. Furthermore, moderately surface-active compounds, such as 2-methylglutaric acid (2-

MGA, Fig. 1, green squares) and sodium octyl sulfate (Fig. 1, grey diamonds), exhibit surface tension depression in the range of ~ 64–$68\,mN\,m^{-1}$ for concentrations $\leq 22\,mM$ (Tables S13–S14). Additionally, stronger surface-active organics (surfactants), such as sodium dodecyl sulfate (SDS), show surface tension at the droplet surface can be depressed in the dilute regime. SDS reaches $\sigma_{s/a}$ of $\sim 39\,mN\,m^{-1}$ at $9\,mM$ organic (Fig. 1 and Table S15). Sodium octyl sulfate, SDS, and 2-MGA present noticeable surface tension depression in the dilute bulk measurement regime (Fig. 1) that affect aerosol properties (Vepsäläinen et al., 2023; Zhang et al., 2023; Kleinheins et al., 2025). However, in comparison to previously studied organics, 2-MT and 2-MTS $\sigma_{s/a}$ samples remain close to pure water in the dilute bulk regime (Fig. 1). Previous studies by Bain et al. (2023) and Werner et al. (2025) emphasize the role of the surface area-to-volume ratio dictating aerosol surface tension. Specifically, aerosol surface tension values are best represented by surface tension measurements of the organic in bulk solutions $< 100\,mM$ (Bain et al., 2023; Ferdousi-Rokib et al., 2025; Werner et al., 2025). Thus, 2-MT and 2-MTS sample mixture surface activity is negligible for droplet activation as dilute organic $\sigma_{s/a}$ is close to that of pure water ($\sim 72\,mN\,m^{-1}$).

It should be reiterated and noted that the synthesized 2-MTS sample is 73 % pure 2-MTS and is likely mixed with AS and SMS. Both SMS and AS (Fig. 1, red circles; Table S16) have surface tension values $> 72\,mN\,m^{-1}$ in the dilute regime. However, despite the presence of impurities in the mixture, synthesized 2-MTS sample mixture surface tension reaches values $\sim 68\,mN\,m^{-1}$. Therefore, the presence of these impurities may counteract possible further surface tension depression exhibited by pure 2-MTS. Future work can better probe surface tension of the pure organic 2-MTS and effects of SMS by applying a multicomponent surface tension model (e.g., multicomponent models of Topping et al., 2007) to dynamic surface tension measurements.

Both 2-MT and 2-MTS are considered viscous compounds and may diffuse slowly through the measured droplets (Reid et al., 2018; Zhang et al., 2019a; Chen et al., 2023). As a result, equilibrium surface tension is reached after a period of time, t. The rate of diffusion of the organic through water, also known as the diffusion coefficient D_s, can be calculated from dynamic surface tension measurements (Eqs. 1–2). Diffusion coefficient values for synthesized 2-MT and 2-MTS samples range between 10^{-9} and $10^{-11}\,m^2\,s^{-1}$, with diffusion slowing with increasing sample concentration. Specifically, D_s for the 2-MT and 2-MTS samples is estimated to be 10^{-9} to 10^{-11} and 10^{-9} to $10^{-10}\,m^2\,s^{-1}$, respectively (Table S17). Additionally, the viscosity-based diffusion coefficient was calculated and shown in Table S19. 2-MT and 2-MTS diffusion rates are comparable to rates observed for other previously investigated viscous components in aqueous solution (Curry et al., 2018; Tandon et al., 2019). For example, methylglyoxal, a known viscous component, has an aqueous-phase diffusion rate $\sim 10^{-9}\,m^{-2}\,s^{-1}$ (Curry et

al., 2018). In addition to the diffusion coefficients in aqueous solution, a study by Chenyakin et al. (2017) showed average diffusion coefficients between 10^{-13} and $10^{-14}\,m^2\,s^{-1}$ for organic molecules in a sucrose–water proxy for SOA. A study by Renbaum-Wolff et al. (2013) reported diffusion coefficients ranging from 10^{-13} and $10^{-15}\,m^2\,s^{-1}$ for α-pinene-derived SOA between 70 %–90 % RH. Indeed, 2-MT and 2-MTS have been previously observed to be highly viscous, resulting in slow diffusivity (Wang et al., 2011; Chenyakin et al., 2017; Tandon et al., 2019; Zhang et al., 2019a; Chen et al., 2023). Furthermore, at higher viscosity and lower diffusion rates, the diffusion of solute molecules fails to follow the Stokes–Einstein relationship describing the self-diffusion of solute molecules through a liquid phase (Einstein, 1905; Chenyakin et al., 2017; Tandon et al., 2019). For viscous material, such as 2-MT and 2-MTS samples, diffusion in water is self-limited (Chenyakin et al., 2017). Slow diffusion correlates with the longer timescales needed to reach equilibrium surface tension for more concentrated sample solutions; the solute molecules are limited in their ability to accumulate to the surface; thus, time is an important factor in the surface tension measurements. This effect is more prominent in the 2-MT than the 2-MTS sample, as evident in its slower diffusion rates for concentrations $> 30\,mM$ (Table S17).

4.1.2 AS and synthesized organic mixture

Previous studies have observed that inorganic compounds, such as AS, mixed with organics can enhance surface tension effects (Topping, 2010; El Haber et al., 2023). Additionally, AS can result in the partitioning of organics to the surface (i.e., the movement of organics to the surface is commonly referred to as salting out). To determine if partitioning effects are present in organic / AS mixtures, synthesized 2-MT and 2-MTS samples were mixed with 500 mM AS, and dynamic surface tension measurements were taken; mixture dynamic surface tension measurements are shown in Fig. 2. Average mixed surface tension values are listed in Table S10.

For mixtures of 3–9 mM 2-MT and 500 mM AS, surface tension remains stable $\sim 75\,mN\,m^{-1}$ and is higher than the 2-MT ($> 98\,wt\%$ purity) solution surface tension alone (Fig. 2a). Higher $\sigma_{s/a}$ values indicate a lack of salting-out effects and organic surface partitioning; previous surface tension studies of organic / AS mixtures observed salting–out effects through lower $\sigma_{s/a}$ values in comparison to pure organic solutions (Ferdousi-Rokib et al., 2025). Thus, for 3–9 mM 2-MT with 500 mM AS mixtures, organic partitioning is not enhanced, and the droplet surface tension aligns with pure AS $\sigma_{s/a}$ (Fig. 1 and Table S16). When organic concentration in the mixture is increased to 94 mM, a stronger time dependence for surface tension is observed (Fig. 2a); an equilibrium surface tension of $\sim 71.2\,mN\,m^{-1}$ is reached at $\sim 300\,s$. This lower surface tension for 94 mM 2-MT with 500 mM AS compared to the previous 2-MT / AS mixture

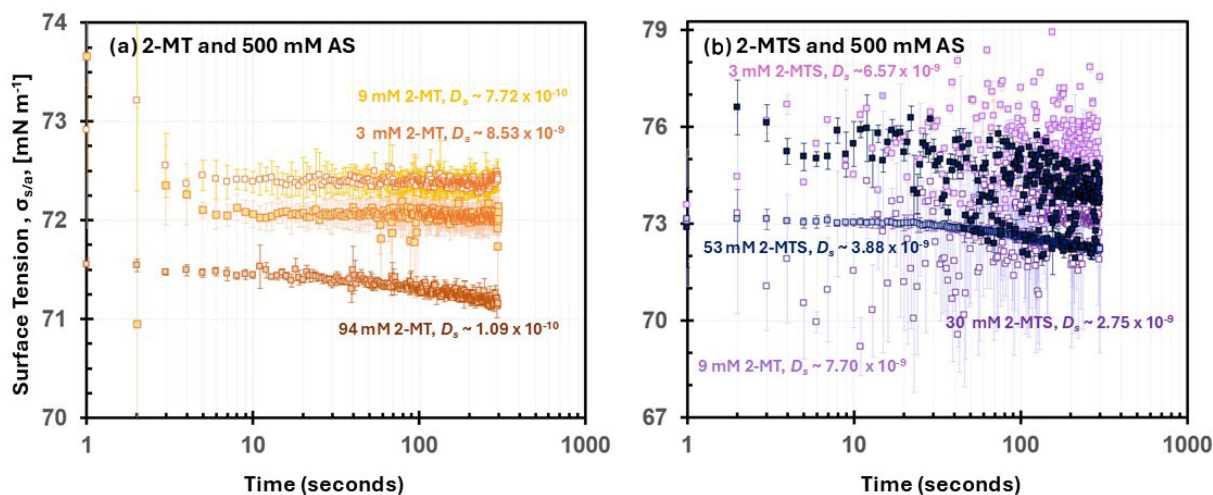**Figure 2.** Dynamic $\sigma_{s/a}$ measurements for **(a)** 3–94 mM 2-MT sample / 500 mM AS and **(b)** 3–53 mM 2-MTS sample / 500 mM AS mixtures. Dynamic $\sigma_{s/a}$ was recorded over a duration of 300 s. The 2-MTS sample mixtures likely contain additional contributions of AS (3 wt %) and SMS (24 wt %), which may further influence dynamic surface tension measurements and overall sample diffusivity.

correlates with the higher concentration of organic in solution. However, the longer equilibrium time is indicative of a slow solute diffusion in the droplet.

Previous studies have observed diffusion effects within dynamic surface tension measurements and estimated solute diffusion (Eastoe et al., 1998; Bain et al., 2024). To determine organic diffusion within AS mixtures, the D_s was calculated using Eqs. (1)–(2). For 2-MT / AS mixtures, D_s ranged from 10^{-9} to 10^{-11}, with diffusion slowing as organic concentration increases (Fig. 2a, Table S17). 2-MT organic diffusion in AS mixtures is similar to that of the organic 2-MT solution (with $> 98\%$ purity) D_s values. As a result, 2-MT organic diffusion remains relatively unaffected in the presence of AS. The organic 2-MT molecules do not diffuse fast enough to fully accumulate at the surface and substantially lower surface tension.

Similar to 2-MT / AS mixtures, 2-MTS / AS mixture surface tension was higher than 2-MTS sample solution surface tension alone. 2-MTS / AS mixture $\sigma_{s/a}$ values ranged from ~ 72.5 to $75 \, \text{mN m}^{-1}$ and remain close to surface tension values of pure AS. Furthermore, $\sigma_{s/a}$ values remain constant as the 2-MTS organic concentration increases from 3 to 53 mM; the minimal correlation between organic concentration and surface tension implies that AS dominates droplet surface tension at the surface–air interface. In addition to being stable across organic concentrations, 2-MTS / AS $\sigma_{s/a}$ reaches equilibrium faster than 2-MT / AS; equilibrium is achieved across the mixtures at $< 100 \, \text{s}$ (Fig. 2b). Indeed, based on the dynamic surface tension measurements, D_s for 2-MTS within AS mixtures remains $\sim 10^{-9}$, indicating slightly faster organic diffusivity through the droplet than 2-MT (Table S17). In the presence of AS, D_s increases by an order of magnitude. This suggests the presence of

AS increases solubility and dispersion of 2-MTS molecules through the droplet (Prisle et al., 2010; Toivola et al., 2017). A similar phenomenon has been observed in glyoxal / AS mixtures as the presence of the inorganic compound improves dissolution of the organic (Kampf et al., 2013). Therefore, the higher 2-MTS / AS surface tension values and diffusivity indicate that the organic is well dispersed within the droplet, but AS dominates droplet surface tension properties. Both 2-MT and 2-MTS present complex viscous properties that may affect droplet phase and potentially change in the presence of inorganic compounds, such as AS. It is important to note that for 2-MTS, the remaining sample mass also contains SMS, which may further influence the estimated diffusion rates (Vignes, 1966; Wallace et al., 2021). Diffusion coefficients within aerosols may be sensitive to mixture ratio, as observed by Wallace et al. (2021). Thus, the presence of SMS may affect the 2-MTS sample / AS diffusion rates observed in this study. Future work should explore the influence of SMS on viscous organic diffusivity by applying this study's methodology to a range of 2-MTS sample / SMS mixtures with 2-MTS contribution greater than 73 wt %. Ultimately, diffusion effects were observed through dynamic surface tension measurements and may influence 2-MT, 2-MTS, and AS-mixed aerosol water uptake properties. Therefore, additional diffusion effects on synthesized organic and organic / AS aerosol mixtures were probed through the lens of water uptake measurements.

4.2 Water uptake measurements

In addition to the previous measurements, the droplet growth of 2-MT and 2-MTS samples and their respective AS mixtures was measured; hygroscopicity was estimated under both subsaturated and supersaturated conditions. Mixtures

were varied by sample wt % (Table S21); organic wt % of 2-MTS is estimated by accounting for impurities present in the sample and their respective properties (e.g., density, hygroscopicity, Table S20). The adjusted mass wt % for 2-MTS / AS mixtures is listed in Table S21. For subsaturated hygroscopicity, the H-TDMA instrument setup was used to measure G_F for all experimental solutions at 88.2 % RH. Experimental growth factor values for 2-MT / AS and 2-MTS / AS mixtures are listed in Tables S20–S21. For supersaturated hygroscopicity, the CCNC instrument setup was used to obtain experimental $D_{p,50}$ values across multiple supersaturation conditions (0.31 %, 0.43 %, 0.65 %, 0.88 %, 1.10 %, 1.32 %, and 1.54 % SS); the critical diameter values for 2-MT / AS and 2-MTS / AS mixtures are listed in Tables S22–S23. For 100 wt % 2-MTS, impurity (SMS and additional AS) and hygroscopicity are accounted for by applying the ZSR mixing rule (Eq. 6) to solve for pure organic hygroscopicity; SMS κ was assumed to be ~ 0.459 based on Peng et al. (2021).

Under subsaturated conditions, both 2-MT and 2-MTS are moderately hygroscopic, with $\kappa_{\text{H-TDMA}}$ values of 0.103 and 0.276, respectively (Fig. 3a). For 2-MT / AS (Fig. 3a, orange open squares) and 2-MTS / AS (Fig. 3a, purple open circles) aerosol mixtures, subsaturated hygroscopicity values are similar. For 2-MT / AS mixtures ≤ 45 wt % organic, κ values plateau close to pure AS ($\kappa_{\text{int}} = 0.61$) at a $\kappa_{\text{H-TDMA}} \sim 0.56$. For mixtures > 45 wt % organic, both 2-MT and 2-MTS exhibit lower $\kappa_{\text{H-TDMA}}$ values, ranging from 0.103–0.505 for 2-MT / AS mixtures and 0.276–0.433 for 2-MTS / AS mixtures. Previous studies by Malek et al. (2023) and Ferdousi-Rokib et al. (2025) have observed a plateau in hygroscopicity for AS-dominated organic mixtures prior to a decrease in κ due to the presence of phase-separated morphology; as a result of phase separation, the inorganic AS remains dissolved in the aqueous phase and drives hygroscopicity (Malek et al., 2023). After a threshold composition is reached (45 wt % organic), more organic solute contributes to the aqueous phase, and thus hygroscopicity is lowered.

Under supersaturated conditions, 2-MT and 2-MTS samples remain moderately hygroscopic, with κ_{CCN} being 0.269 and 0.139, respectively. For 2-MT / AS sample mixtures (Fig. 3b, closed orange squares), supersaturated κ mimics the same trend as subsaturated 2-MT / AS κ; for mixtures ≤ 60 wt % 2-MT, κ_{CCN} also shows a plateau at ~ 0.53 and then decreases with increased organic aerosol composition. In comparison, the 2-MTS / AS sample mixtures (Fig. 3b, purple circles) present a linear hygroscopic trend; as organic wt % increases, κ_{CCN} drops in a linear fashion resembling ideal mixing and volume additivity (Petters and Kreidenweis, 2007). Indeed, 2-MTS / AS κ_{CCN} correlates with the hygroscopicity trend predicted by κ_{ZSR} values (Eqs. 11–12) (Fig. 3b, purple line). 2-MTS / AS supersaturated hygroscopicity agrees well with original Köhler theory ($R^2 = 0.972$, Table S26), suggesting full 2-MTS dissolution and contribution to water uptake. By contrast, 2-MT / AS mix-

tures do not agree with κ-Köhler theory ($R^2 = 0.787$, Table S26), with the greatest discrepancy observed in the region between the κ experimental plateau and κ_{ZSR} (Fig. 3, orange line); additionally, subsaturated 2-MTS / AS mixtures deviate from κ_{ZSR} during the initial hygroscopic plateau (Fig. 3a, purple line). Thus, for 2-MT / AS mixtures and subsaturated 2-MTS / AS aerosols, the ideal volume additive mixing rule does not apply. This can once again be attributed to limitations to organic dissolution into the aqueous phase (Malek et al., 2023). For 2-MTS / AS sample mixtures, both subsaturated and supersaturated hygroscopic trends may be further impacted by the presence by SMS. The contributions of AS and SMS hygroscopicity are accounted for 2-MTS sample mixture. κ was estimated using the ZSR mixing rule, which assumes ideal interactions between SMS, AS, and 2-MTS. However, non-idealities (e.g., phase separation, salting in) may result in SMS having a greater influence on hygroscopicity and can be the focus of future exploration.

In addition to non-ideal hygroscopic trends, it is noted that overall, κ_{CCN} values remain lower than $\kappa_{\text{H-TDMA}}$ values for both 2-MT / AS and 2-MTS / AS sample mixtures, contrary to the usual trend of $\kappa_{\text{CCN}} > \kappa_{\text{H-TDMA}}$ (Petters and Kreidenweis, 2007). The observed difference suggests greater organic dissolution and contribution to hygroscopicity in the supersaturated regime compared to subsaturated conditions. This suggests potential viscosity and diffusion limitations on hygroscopicity as RH transitions from sub- to supersaturated. Indeed, the viscosity of the 2-MT and 2-MTS changes under different conditions. Both compounds remain in the semi-solid phase state before entering the CCNC and behave like liquids in the H-TDMA, as shown in Table S18. Additionally, Asa-Awuku and Nenes (2007) report diffusivity limitation effects on aerosol water uptake for compounds with D_s values $\leq 2.5 \times 10^{-10}$, well within the range of D_s values for 2-MT, and 2-MT sample / AS. Water uptake was shown to be driven by the viscous organic phase slowly diffusing into the aqueous phase (Asa-Awuku and Nenes, 2007). Thus, it is believed that both 2-MT and 2-MTS slowly dissolve and phase separate to form a viscous phase under subsaturated conditions, corresponding to slow diffusion coefficients. AS is an inorganic compound that is assumed to instantaneously dissolve into the aqueous phase and thus drives hygroscopicity when the droplet is phase separated, such as for 2-MT / AS mixtures (Fig. 2). However, lower κ values at supersaturated conditions can be attributed to higher water content; previous studies have found greater water content correlating with reduced viscosity due to a plasticizing effect and resulting in enhanced organic mixing (O'Meara et al., 2016; Reid et al., 2018; Jeong et al., 2022). Thus, the organic viscous phase may experience "cracking" and greater movement of organic molecules through the aqueous phase (Tandon et al., 2019). Therefore, phase behavior of the organic can have a strong influence on aerosol water uptake. Additionally, the non-ideal hygroscopic behavior of 2-MT / AS and subsaturated 2-MTS / AS mixtures versus the ideal hygroscopic be-
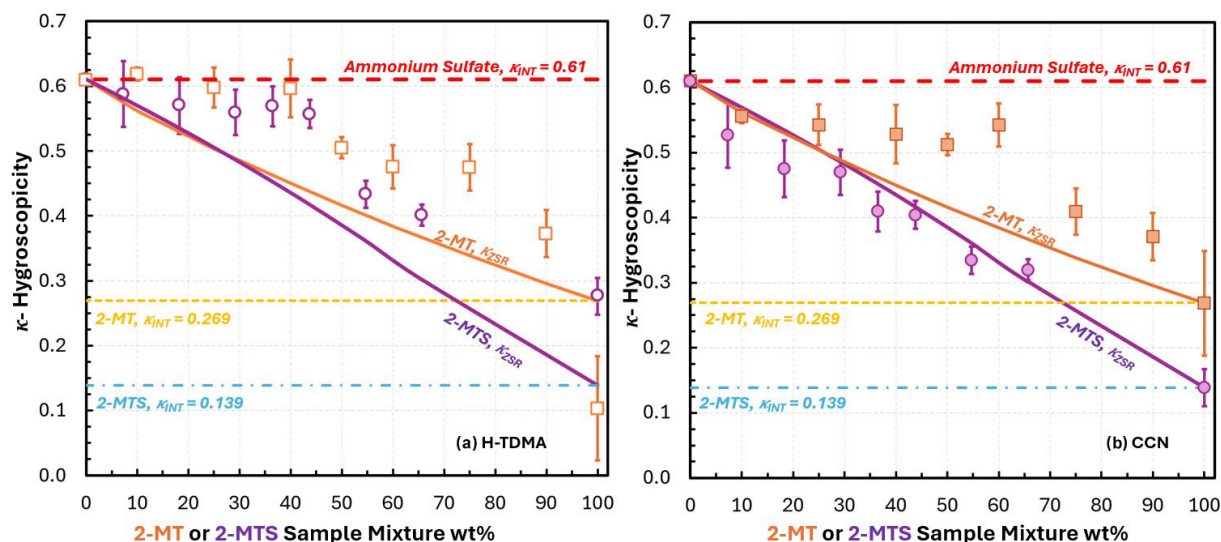
Figure 3. Experimental κ-hygroscopicity measurements derived from **(a)** H-TDMA measurements and **(b)** CCNC measurements. 2-MTS / AS sample mixture wt % was adjusted based on the presence of AS and SMS impurities (Table S21). Subsaturated hygroscopicity ($\kappa_{\text{H-TDMA}}$) of 2-MT / AS and 2-MTS / AS sample mixtures are represented as open orange squares and open purple circles, respectively. Supersaturated hygroscopicity (κ_{CCN}) for 2-MT / AS and 2-MTS sample / AS mixtures are represented as orange squares and purple circles, respectively. For 100 wt % 2-MTS, κ values were adjusted to account for impurities by applying mixing rule, assuming an SMS κ of ~ 0.459 and AS $\kappa \sim 0.61$ (Eq. 6, Table S20). κ-Köhler theory (κ_{ZSR}) was used to predict hygroscopicity of 2-MT / AS (solid orange line) and 2-MTS sample/AS (solid purple line) via Eq. (6). Organic κ_{int} was determined from 100 wt % κ_{CCN}. 2-MT κ_{int} (yellow dashed line) was determined to be 0.269. 2-MTS κ_{int} (blue dashed line) was determined to be 0.139.

havior of supersaturated 2-MTS / AS aerosols can be probed through imaging of the aerosol mixture phase behavior.

4.3 Phase morphology

To further understand the phase state and morphology of 2-MT and 2-MTS sample mixtures with AS, AFM images were taken at varied organic wt % (Fig. 4). Dried synthesized 2-MTS presents itself as a viscous, spherical particle, indicated by its smooth surface (Fig. S4); this agrees with both shape factor measurement of ~ 1 (Armstrong et al., 2025) and diffusion coefficient values. As inorganic AS is mixed with 2-MTS sample, phase behavior changes. At 10 wt % 2-MTS sample (Fig. 4b), particles exhibit an engulfed core–shell morphology. A previous study by Cooke et al. (2022) observed a similar core–shell morphology for AS-seeded IEPOX-derived SOA particles; the study observed an organic shell, while the inorganic salt was observed to be present in the shell as well as within an aqueous core (Cooke et al., 2022). With AS dispersed on the outer shell as well as being present in an aqueous core, the inorganic salt in the shell will likely easily dissolve during water uptake and drive hygroscopicity, consistent with the results as observed in subsaturated hygroscopicity measurements. However, AS within the shell may introduce roughness in the outer edge which can promote "cracking" in the organic phase, which can result in full dissolution in the presence of higher water content and ideal mixing (Tandon et al., 2019).

As 2-MTS is increased to 45 wt %, the particle morphology shows greater inorganic phase dispersion, with AS protruding through the viscous organic phase (Fig. 4c). The visualized morphology and phase state of the particle agree with behavior inferred from water-uptake and droplet measurements (Sect. 4.2). In particular, ~ 45 wt % is the observed threshold for the plateau in 2-MTS / AS $\kappa_{\text{H-TDMA}}$ values, prior to a linear decrease in $\kappa_{\text{H-TDMA}}$ values. The dispersion of AS disrupts the organic network within the viscous phase, giving rise to the observed roughness and promoting the salting in of 2-MTS. This phenomenon agrees with the results of previously published literature that show viscous organics mixed with AS, specifically, laboratory-generated SOA–AS and citric acid–AS mixtures (Saukko et al., 2012; Abramson et al., 2013). Previous studies have also observed increased diffusion within viscous SOA particles via a disruption of the hydrogen bonding network between the organic molecules that can promote solute movement in the droplet (Reid et al., 2018; Jeong et al., 2022; Sheldon et al., 2023). For this reason, it is likely that greater organic diffusion occurs above 45 wt % organic, resulting in decreasing $\kappa_{\text{H-TDMA}}$ values. Furthermore, the well-dispersed AFM morphology is indicative of ideal mixing under supersaturated conditions, thereby agreeing with κ-Köhler theory of droplet growth.

In comparison, 2-MT mixtures present an engulfed core–shell morphology from 10 wt % to 45 wt % organic (Fig. 4d–e). At 10 wt % 2-MT, the viscous organic phase dominates
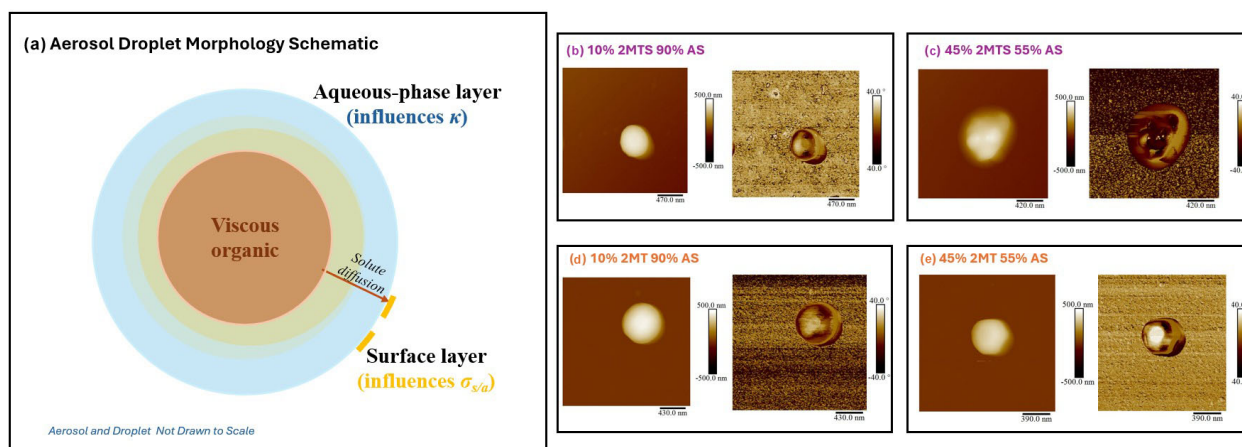
Figure 4. (a) Schematic depicting aerosol droplet composed of a viscous organic core and aqueous-phase layer and AFM images of **(b)** 10 wt % 2-MTS–90 wt % AS, **(c)** 45 wt % 2-MTS–55 wt % AS, **(d)** 10 wt % 2-MT–90 wt % AS, and **(e)** 45 wt % 2-MT–90 wt % AS. AFM results depict vertical particle height (left) and phase morphology (right).

the particle morphology and AS remains dispersed at the surface edge, as shown in Fig. 4d. As organic wt % increases to 45 wt %, morphology remains unchanged and the organic phase stays intact. The intact core–shell morphology of 45 wt % 2-MT aerosol mimics contrasts with the well-dispersed morphology observed for 45 wt % 2-MTS aerosol mimic. For 2-MT, the organic diffusion is limited under both sub- and supersaturated conditions, likely due to the undissolved viscous organic phase (Fig. 4a). Specifically, 2-MT viscosity causes slower dissolution compared to AS and results in the phase-separated morphology. Thus, hygroscopicity of the 2-MT / AS mixture is dominated by AS dissolution from the core and outer shell, corresponding to the hygroscopic plateau observed for 2-MT / AS sub- and supersaturated water uptake measurements (Fig. 3). Therefore, particle morphology and viscosity influence the synthesized 2-MT's ability to diffuse through the aerosol droplet and can affect aerosol water uptake process. Indeed, a previous study by Zhang et al. (2018) described the self-limiting effect of a core–shell morphology on IEPOX-SOA reactive uptake and can now be observed in the 2-MT / AS water uptake process. However, diffusion limitations can also result in the need for longer time periods to reach an equilibrium state, as observed by dynamic surface tension measurements. Consequently, current hygroscopicity measurements that occur at fast timescales may not capture the full water uptake process of the synthesized organics and their mixtures. For example, the residence of aerosols within DMT CCNC columns is ∼ 10 s (Paramonov et al., 2015), while similar H-TDMA instrument setups have a residence time ∼ 6.5 s (Mikhailov and Vlasenko, 2020). However, a previous study by Chuang (2003) found atmospheric droplet growth timescales range between 5 and 100 s, congruent with the timescale of 2-MT and 2-MTS dynamic surface tension change (Fig. 2 and Chuang, 2003). Therefore, the hygroscopicity of viscous-

organic-containing aerosols, such as 2-MT and 2-MTS, must be studied at greater residence times to observe any possible effects on hygroscopicity; understanding whether timescale affects CCN activity of organic–inorganic aerosol mixtures can greatly impact current global models that may assume instantaneous solute dissolution during the water uptake process. Furthermore, future studies should consider whether the hygroscopicity approximations of viscous 2-MT / AS and 2-MTS / AS mixtures are time dependent, as time-dependent droplet formation has been observed for biogenic aerosols (Vizenor and Asa-Awuku, 2018). Currently, traditional κ-Köhler theory is unable to predict the water uptake of 2-MT / AS and subsaturated 2-MTS / AS aerosols and does not consider solute and droplet kinetic effects. However, by accounting for phase morphology and viscosity, κ predictions may be improved.

In addition, size-dependent morphology may also affect κ-hygroscopicity estimations. Several studies observe a relationship between particle size and aerosol phase transitions during water uptake (Veghte et al., 2013; Cheng et al., 2015; Altaf et al., 2016; Schmedding and Zuend, 2025). Specifically, Veghte et al. (2013) and Cheng et al. (2015) observe smaller AS–organic particles, favoring a homogeneous liquid phase, while larger particles remain in a partially engulfed morphology; this finding correlates with 2-MT / AS engulfed morphology for particles imaged ≥ 390 nm (Fig. 4). Indeed, for 2-MT / AS mixtures > 60 wt % 2-MT, κ_{CCN} decreases with increasing dry activation diameter before plateauing (Fig. S5). This trend may correlate to greater organic diffusion as particle size and morphology changing before a dissolution limit is reached for > 60 wt % 2-MT / AS mixtures. For mixtures ≤ 60 wt % 2-MT, a similar decrease in κ_{CCN} is observed before hygroscopicity begins to increase; this may be attributed to the engulfed morphology in larger particles (Fig. 4d–e) promoting AS dissolution and water

uptake contribution while 2-MT diffusion reaches a limit. However, the water uptake measurements performed in this study do not account for size-dependent phase morphology in its analysis. Therefore, future work may build upon the results of this study to better parameterize hygroscopicity based on initial particle size and size-dependent phase morphology affecting κ-hygroscopicity estimations. In particular, size-selected CCN measurements can be performed to better probe size-dependent morphology effects on aerosol activation. By doing so, global models can incorporate these influential physicochemical properties into predictions of aerosol–cloud interactions.

5   Summary and implications

In this study, we investigated the influence of solute diffusivity and droplet phase morphology on the hygroscopicity of synthesized 2-MT and 2-MTS samples and their mixtures with AS. Mixtures with AS were varied by organic wt %. Both 2-MT and 2-MTS were previously observed to be viscous and glassy, affecting diffusivity through water. Additionally, previous studies found 2-MT to be weakly surface active. To determine organic diffusivity and potential surface activity, dynamic surface tension measurements were taken for aqueous organic and mixed organic–inorganic solutions. 2-MT and 2-MTS were found to be weakly surface active. Previous studies by Bain et al. (2023) and Mikhailov et al. (2024) determined that surface activity in the dilute bulk concentration range correlates with depressed aerosol surface tension. However, neither the 2-MT sample nor the 2-MTS sample is sufficiently surface active to depress droplet surface tension at the air–surface interface. 2-MT and 2-MTS sample solutes move slowly in droplets and have estimated diffusion rates (D_s) between 10^{-9} and $10^{-11}\,\mathrm{m^2\,s^{-1}}$, with diffusion slowing as organic concentration is increased. When mixed with AS, 2-MT diffusivity remains slow ($10^{-10}\,\mathrm{m^2\,s^{-1}}$), while 2-MTS diffusivity increases by an order of magnitude ($10^{-9}\,\mathrm{m^2\,s^{-1}}$); 2-MTS diffusion in aqueous AS mixtures is similar to other quickly dissolving compounds, such as NaCl ($D_s = 10^{-9}$, Vitagliano and Lyons, 1956; Leaist and Hao, 1992) and can result in a well-mixed droplet.

Organic viscosity and diffusion affect aerosol water uptake (Asa-Awuku and Nenes, 2007; Bones et al., 2012; Tandon et al., 2019). For 2-MT and 2-MTS samples and subsequent mixtures under both sub- and supersaturated conditions, droplet growth is affected by solute diffusion. Subsaturated droplet growth was measured using a H-TDMA at 88.2 % RH, and subsaturated hygroscopicity was parameterized by $\kappa_{\mathrm{H\text{-}TDMA}}$. For supersaturated conditions, a CCNC determined the activation ratio of particles at varied supersaturations (0.3 %–1.4 % SS) and water uptake was parameterized by κ_{CCN}. 2-MT / AS mixtures exhibit plateaued $\kappa_{\mathrm{H\text{-}TDMA}}$ and κ_{CCN} values close to κ_{int} of AS (~ 0.61). A similar plateau behavior is observed for 2-MTS / AS $\kappa_{\mathrm{H\text{-}TDMA}}$.

However, for supersaturated conditions, 2-MTS / AS mixture κ_{CCN} follows ideal mixing behavior, represented by its proximity to κ-hygroscopicity predicted by κ-Köhler theory and volume additive ZSR. Additionally, $\kappa_{\mathrm{H\text{-}TDMA}}$ remains higher than κ_{CCN}; this is a result of increased water content reducing viscosity effects and enhancing organic dissolution under supersaturated conditions.

The κ-hygroscopicity plateau in Fig. 3 has been previously attributed to the presence of phase separation, resulting in the inorganic, more soluble, and ideal compound (AS) driving water uptake (Malek et al., 2023). However, for 2-MTS / AS, ideal hygroscopic behavior is indicative of a well-dissolved, homogeneous droplet (Petters and Kreidenweis, 2007). To better understand phase morphology of the synthesized organic / AS mixed particles, AFM measurements of synthesized 2-MTS, 2-MTS / AS mixtures, and 2-MT / AS mixtures were acquired. 2-MTS aerosols are smooth, spherical, viscous particles; when mixed with AS at 10 wt %, AS remains in the aqueous core and is dispersed on the side of the particle, introducing roughness on the aerosol outer shell. As organic concentration increases, the AS core is broken up through the particle. The less defined core–shell morphology may be the result of AS disrupting the interactions between neighboring 2-MTS particles in the viscous network; as a result, organic dissolution becomes faster as indicated by greater 2-MTS diffusion rates. Thus, 2-MTS sample/AS aerosols behave similar to traditional full dissolution assumptions. In comparison, 2-MT / AS mixture AFM images show an engulfed core–shell morphology regardless of organic concentration. As a result, the viscous organic phase remains intact, while aqueous AS in the core drives hygroscopicity. A caveat to these results is the presence of SMS, an organosulfate, being present within the 2-MTS sample at ~ 24 wt %. Therefore, SMS may have an effect on surface tension, diffusivity, and hygroscopic trends observed for the 2-MTS sample / AS mixtures that is currently unknown in this study. Future work may utilize the methodology laid out in this work to more deeply probe the influence of SMS and any additional mixture component on viscous organic properties and water uptake.

This study demonstrates that viscosity can dictate organic diffusion through aqueous droplets, resulting in complex phase morphology and water uptake properties. Furthermore, the synthesized samples studied in this work are representative of the hygroscopic properties of IEPOX-SOA mixtures. A recent study by Armstrong et al. (2025) determined that the IEPOX-SOA composition is composed of a range of 2-MT, 2-MTS, and additional components that vary with aerosol acidity. Thus, the synthesized samples present in this work may present a subset of SOA aerosols generated and this study provides insight into its potential diffusive, hygroscopic, and phase behavior. For example, as shown by this study's water uptake measurements, hygroscopicity from the subsaturated to supersaturated regime evolves due to the presence of increased water content. However,

it is also noted that the hygroscopicity measurements performed in this study were on short timescales (6–10 s); in comparison, dynamic surface tension measurements showed droplet equilibrium being reached at 100–300 s for aqueous 2-MT, 2-MT / AS, and 2-MTS. Thus, current water uptake measurements may not capture a potentially evolving hygroscopicity over time. This is critical in understanding biogenic aerosol influence on cloud formation; a previous study by Chuang (2003) found that droplet formation can occur within timescales of 5–100 s, well within evolving diffusion times observed in this study. Therefore, future work must investigate potentially dynamic water uptake of viscous biogenic aerosols, such as 2-MT and 2-MTS. Furthermore, time-dependent κ can be developed to better account for organic diffusion within larger-scale cloud parcel and global models. In addition to time dependency, κ-hygroscopicity estimations may also be affected by size dependent phase morphology. A study by Veghte et al. (2013) found smaller aerosol particles preferring a homogenous state, while larger particles have an engulfed core–shell morphology similar to 2-MT / AS aerosols in this study. Therefore, particle size may influence viscous organic / AS water uptake due to diffusion and morphological influences. Future work may explore and parameterize the effect of size-dependent phase-separated morphology on aerosol activation through step size-selected CCN measurements. Ultimately, it is crucial to understand how the properties (viscosity, diffusivity, and phase morphology) of biogenic aerosols, such as 2-MT and 2-MTS, alter cloud formation. The results of this study demonstrate the co-dependency of these properties for two isoprene-derived compounds and thus may improve our overall understanding of how biogenic aerosols and their mixtures affect aerosol–cloud interactions.

Code availability. PyCAT code is available for public use through Zenodo at https://doi.org/10.5281/zenodo.6329787 (Gohil, 2022).

Data availability. Data sets are available in the Supplement as well as in a data repository at https://doi.org/10.13016/o6uq-7tac (Ferdousi-Rokib, 2025).

Supplement. The supplement related to this article is available online at https://doi.org/10.5194/acp-25-15613-2025-supplement.

Author contributions. NFR designed, collected, and analyzed all experimental data and analyzed theoretical models. NCA contributed to design and analysis of water uptake data. SJ contributed to design and collection of H-TDMA experimental data. AJD contributed to design and analysis of AFM data. MA contributed to design and collection of AFM data. ERR contributed to collection of surface tension experimental data. ZZ and AG contributed to sample synthesis. JLW contributed to design, collection, and analysis of

dynamic surface tension experimental data. YZ contributed to viscosity, diffusion, and AFM data analysis. All authors contributed to the writing and preparation of the manuscript.

Disclaimer. Publisher's note: Copernicus Publications remains neutral with regard to jurisdictional claims made in the text, published maps, institutional affiliations, or any other geographical representation in this paper. While Copernicus Publications makes every effort to include appropriate place names, the final responsibility lies with the authors. Views expressed in the text are those of the authors and do not necessarily reflect the views of the publisher.

Review statement. This paper was edited by Daniel Knopf and reviewed by two anonymous referees.

References

Abramson, E., Imre, D., Beránek, J., Wilson, J., and Zelenyuk, A.: Experimental determination of chemical diffusion within secondary organic aerosol particles, Phys. Chem. Chem. Phys., 15, 2983–2991, https://doi.org/10.1039/C2CP44013J, 2013.

Albrecht, B. A.: Aerosols, Cloud Microphysics, and Fractional Cloudiness, Science, 245, 1227–1230, https://doi.org/10.1126/science.245.4923.1227, 1989.

Altaf, M. B., Zuend, A., and Freedman, M. A.: Role of nucleation mechanism on the size dependent morphology of organic aerosol, Chemical Communications, 52, 9220–9223, https://doi.org/10.1039/C6CC03826C, 2016.

Armstrong, N. C., Gagan, S., Dodero, A. J., Ferdousi-Rokib, N., Frauenheim, M., Gold, A., Zhang, Z., Asa-Awuku, A., Zhang, Y., and Surratt, J. D.: Hygroscopicity Depends on Aerosol Acidity and Sulfate Content during the Reactive Uptake of Isoprene

Epoxydiols, ACS Earth and Space Chemistry, 9, 2324–2335, https://doi.org/10.1021/acsearthspacechem.5c00163, 2025.

Asa-Awuku, A. and Nenes, A.: Effect of solute dissolution kinetics on cloud droplet formation: Extended Köhler theory, J. Geophys. Res.-Atmos., 112, https://doi.org/10.1029/2005JD006934, 2007.

Bain, A., Ghosh, K., Prisle, N. L., and Bzdek, B. R.: Surface-Area-to-Volume Ratio Determines Surface Tensions in Microscopic, Surfactant-Containing Droplets, ACS Central Science, 9, 2076–2083, https://doi.org/10.1021/acscentsci.3c00998, 2023.

Bain, A., Lalemi, L., Croll Dawes, N., Miles, R. E. H., Prophet, A. M., Wilson, K. R., and Bzdek, B. R.: Surfactant Partitioning Dynamics in Freshly Generated Aerosol Droplets, J. Am. Chem. Soc., 146, 16028–16038, https://doi.org/10.1021/jacs.4c03041, 2024.

Beier, T., Cotter, E. R., Galloway, M. M., and Woo, J. L.: In Situ Surface Tension Measurements of Hanging Droplet Methylglyoxal/Ammonium Sulfate Aerosol Mimics under Photooxidative Conditions, ACS Earth and Space Chemistry, 3, 1208–1215, https://doi.org/10.1021/acsearthspacechem.9b00123, 2019.

Bertram, A. K., Martin, S. T., Hanna, S. J., Smith, M. L., Bodsworth, A., Chen, Q., Kuwata, M., Liu, A., You, Y., and Zorn, S. R.: Predicting the relative humidities of liquid-liquid phase separation, efflorescence, and deliquescence of mixed particles of ammonium sulfate, organic material, and water using the organic-to-sulfate mass ratio of the particle and the oxygen-to-carbon elemental ratio of the organic component, Atmos. Chem. Phys., 11, 10995–11006, https://doi.org/10.5194/acp-11-10995-2011, 2011.

Bondy, A. L., Bonanno, D., Moffet, R. C., Wang, B., Laskin, A., and Ault, A. P.: The diverse chemical mixing state of aerosol particles in the southeastern United States, Atmos. Chem. Phys., 18, 12595–12612, https://doi.org/10.5194/acp-18-12595-2018, 2018.

Bones, D. L., Reid, J. P., Lienhard, D. M., and Krieger, U. K.: Comparing the mechanism of water condensation and evaporation in glassy aerosol, P. Natl. Acad. Sci. USA, 109, 11613–11618, https://doi.org/10.1073/pnas.1200691109, 2012.

Chan, M. N., Surratt, J. D., Claeys, M., Edgerton, E. S., Tanner, R. L., Shaw, S. L., Zheng, M., Knipping, E. M., Eddingsaas, N. C., Wennberg, P. O., and Seinfeld, J. H.: Characterization and Quantification of Isoprene-Derived Epoxydiols in Ambient Aerosol in the Southeastern United States, Environ. Sci. Technol., 44, 4590–4596, https://doi.org/10.1021/es100596b, 2010.

Chen, B., Mirrielees, J. A., Chen, Y., Onasch, T. B., Zhang, Z., Gold, A., Surratt, J. D., Zhang, Y., and Brooks, S. D.: Glass Transition Temperatures of Organic Mixtures from Isoprene Epoxydiol-Derived Secondary Organic Aerosol, J. Phys. Chem. A, 127, 4125–4136, https://doi.org/10.1021/acs.jpca.2c08936, 2023.

Chen, Y., Dombek, T., Hand, J., Zhang, Z., Gold, A., Ault, A. P., Levine, K. E., and Surratt, J. D.: Seasonal Contribution of Isoprene-Derived Organosulfates to Total Water-Soluble Fine Particulate Organic Sulfur in the United States, ACS Earth and Space Chemistry, 5, 2419–2432, https://doi.org/10.1021/acsearthspacechem.1c00102, 2021.

Cheng, Y., Su, H., Koop, T., Mikhailov, E., and Pöschl, U.: Size dependence of phase transitions in aerosol nanoparticles, Nat. Commun., 6, 5923, https://doi.org/10.1038/ncomms6923, 2015.

Chenyakin, Y., Ullmann, D. A., Evoy, E., Renbaum-Wolff, L., Kamal, S., and Bertram, A. K.: Diffusion coefficients of or-ganic molecules in sucrose–water solutions and comparison with Stokes–Einstein predictions, Atmos. Chem. Phys., 17, 2423–2435, https://doi.org/10.5194/acp-17-2423-2017, 2017.

Chernyshev, V. S. and Skliar, M.: Diffusivity Measurements of Solutes Impacting Interfacial Tension, Industrial & Engineering Chemistry Research, 54, 4535–4544, https://doi.org/10.1021/ie504355w, 2015.

Chuang, P. Y.: Measurement of the timescale of hygroscopic growth for atmospheric aerosols, J. Geophys. Res.-Atmos., 108, https://doi.org/10.1029/2002JD002757, 2003.

Claeys, M., Graham, B., Vas, G., Wang, W., Vermeylen, R., Pashynska, V., Cafmeyer, J., Guyon, P., Andreae, M. O., Artaxo, P., and Maenhaut, W.: Formation of Secondary Organic Aerosols Through Photooxidation of Isoprene, Science, 303, 1173–1176, https://doi.org/10.1126/science.1092805, 2004.

Cooke, M. E., Armstrong, N. C., Lei, Z., Chen, Y., Waters, C. M., Zhang, Y., Buchenau, N. A., Dibley, M. Q., Ledsky, I. R., Szalkowski, T., Lee, J. Y., Baumann, K., Zhang, Z., Vizuete, W., Gold, A., Surratt, J. D., and Ault, A. P.: Organosulfate Formation in Proxies for Aged Sea Spray Aerosol: Reactive Uptake of Isoprene Epoxydiols to Acidic Sodium Sulfate, ACS Earth and Space Chemistry, 6, 2790–2800, https://doi.org/10.1021/acsearthspacechem.2c00156, 2022.

Cope, J. D., Abellar, K. A., Bates, K. H., Fu, X., and Nguyen, T. B.: Aqueous Photochemistry of 2-Methyltetrol and Erythritol as Sources of Formic Acid and Acetic Acid in the Atmosphere, ACS Earth and Space Chemistry, 5, 1265–1277, https://doi.org/10.1021/acsearthspacechem.1c00107, 2021.

Cui, T., Zeng, Z., dos Santos, E. O., Zhang, Z., Chen, Y., Zhang, Y., Rose, C. A., Budisulistiorini, S. H., Collins, L. B., Bodnar, W. M., de Souza, R. A. F., Martin, S. T., Machado, C. M. D., Turpin, B. J., Gold, A., Ault, A. P., and Surratt, J. D.: Development of a hydrophilic interaction liquid chromatography (HILIC) method for the chemical characterization of water-soluble isoprene epoxydiol (IEPOX)-derived secondary organic aerosol, Environmental Science: Processes & Impacts, 20, 1524–1536, https://doi.org/10.1039/C8EM00308D, 2018.

Curry, L. A., Tsui, W. G., and McNeill, V. F.: Technical note: Updated parameterization of the reactive uptake of glyoxal and methylglyoxal by atmospheric aerosols and cloud droplets, Atmos. Chem. Phys., 18, 9823–9830, https://doi.org/10.5194/acp-18-9823-2018, 2018.

Cziczo, D. J., Nowak, J. B., Hu, J. H., and Abbatt, J. P. D.: Infrared spectroscopy of model tropospheric aerosols as a function of relative humidity: Observation of deliquescence and crystallization, J. Geophys. Res.-Atmos., 102, 18843–18850, https://doi.org/10.1029/97JD01361, 1997.

DeCarlo, P. F., Slowik, J. G., Worsnop, D. R., Davidovits, P., and Jimenez, J. L.: Particle Morphology and Density Characterization by Combined Mobility and Aerodynamic Diameter Measurements. Part 1: Theory, Aerosol Sci. Technol., 38, 1185–1205, https://doi.org/10.1080/027868290903907, 2004.

DeRieux, W.-S. W., Li, Y., Lin, P., Laskin, J., Laskin, A., Bertram, A. K., Nizkorodov, S. A., and Shiraiwa, M.: Predicting the glass transition temperature and viscosity of secondary organic material using molecular composition, Atmos. Chem. Phys., 18, 6331–6351, https://doi.org/10.5194/acp-18-6331-2018, 2018.

Eastoe, J., Dalton, J. S., Rogueda, P. G. A., and Griffiths, P. C.: Evidence for Activation-Diffusion Controlled Dynamic Surface

Tension with a Nonionic Surfactant, Langmuir, 14, 979–981, https://doi.org/10.1021/la971241w, 1998.

Einstein, A.: Über die von der molekularkinetischen Theorie der Wärme geforderte Bewegung von in ruhenden Flüssigkeiten suspendierten Teilchen, Annalen der Physik, 322, 549–560, https://doi.org/10.1002/andp.19053220806, 1905.

Ekström, S., Nozière, B., and Hansson, H.-C.: The Cloud Condensation Nuclei (CCN) properties of 2-methyltetrols and C3-C6 polyols from osmolality and surface tension measurements, Atmos. Chem. Phys., 9, 973–980, https://doi.org/10.5194/acp-9-973-2009, 2009.

El Haber, M., Ferronato, C., Giroir-Fendler, A., Fine, L., and Nozière, B.: Salting out, non-ideality and synergism enhance surfactant efficiency in atmospheric aerosols, Sci. Rep., 13, 20672, https://doi.org/10.1038/s41598-023-48040-5, 2023.

Ferdousi-Rokib, N.: Data Set for Hygroscopicity of Isoprene-Derived Secondary Organic Aerosol Mixture Proxies: Importance of Solute Diffusion and Salting-In Effects, DRUM [data set], https://doi.org/10.13016/o6uq-7tac, 2025.

Ferdousi-Rokib, N., Malek, A. K., Mitchell, I. M., Fierce, L., and Asa-Awuku, A. A.: Aerosol Hygroscopicity and Surface-Active Coverage for the Droplet Growth of Aerosol Mixtures, ACS ES&T Air, 2, 1454–1467, https://doi.org/10.1021/acsestair.4c00303, 2025.

Fertil, D., Pierre-Louis, K., Ingwer, S., Galloway, M. M., and Woo, J. L.: Surfactant Effects in Irradiated, Hanging-Droplet, Aqueous-Phase Glyoxal/Ammonium Sulfate Aerosol Mimic Systems, ACS Earth and Space Chemistry, 9, 524–532, https://doi.org/10.1021/acsearthspacechem.4c00288, 2025.

Fordham, S. and Freeth, F. A.: On the calculation of surface tension from measurements of pendant drops, P. Roy. Soc. Lond. A., 194, 1–16, https://doi.org/10.1098/rspa.1948.0063, 1948.

Freedman, M. A.: Phase separation in organic aerosol, Chem. Soc. Rev., 46, 7694–7705, https://doi.org/10.1039/C6CS00783J, 2017.

Froyd, K. D., Murphy, S. M., Murphy, D. M., de Gouw, J. A., Eddingsaas, N. C., and Wennberg, P. O.: Contribution of isoprene-derived organosulfates to free tropospheric aerosol mass, P. Natl. Acad. Sci. USA, 107, 21360–21365, https://doi.org/10.1073/pnas.1012561107, 2010.

Fuchs, N. A.: On the stationary charge distribution on aerosol particles in a bipolar ionic atmosphere, Geofisica pura e applicata, 56, 185–193, https://doi.org/10.1007/BF01993343, 1963.

Gaston, C. J., Riedel, T. P., Zhang, Z., Gold, A., Surratt, J. D., and Thornton, J. A.: Reactive Uptake of an Isoprene-Derived Epoxydiol to Submicron Aerosol Particles, Environ. Sci. Technol., 48, 11178–11186, https://doi.org/10.1021/es5034266, 2014.

Gohil, K.: kgohil27/PyCAT: v1.0, Version v1.0, Zenodo [code], https://doi.org/10.5281/zenodo.6329787, 2022.

Gohil, K. and Asa-Awuku, A. A.: Cloud condensation nuclei (CCN) activity analysis of low-hygroscopicity aerosols using the aerodynamic aerosol classifier (AAC), Atmos. Meas. Tech., 15, 1007–1019, https://doi.org/10.5194/amt-15-1007-2022, 2022.

Guenther, A. B., Jiang, X., Heald, C. L., Sakulyanontvittaya, T., Duhl, T., Emmons, L. K., and Wang, X.: The Model of Emissions of Gases and Aerosols from Nature version 2.1 (MEGAN2.1): an extended and updated framework for modeling biogenic emissions, Geosci. Model Dev., 5, 1471–1492, https://doi.org/10.5194/gmd-5-1471-2012, 2012.

Hettiyadura, A. P. S., Al-Naiema, I. M., Hughes, D. D., Fang, T., and Stone, E. A.: Organosulfates in Atlanta, Georgia: anthropogenic influences on biogenic secondary organic aerosol formation, Atmos. Chem. Phys., 19, 3191–3206, https://doi.org/10.5194/acp-19-3191-2019, 2019.

Hughes, D. D., Christiansen, M. B., Milani, A., Vermeuel, M. P., Novak, G. A., Alwe, H. D., Dickens, A. F., Pierce, R. B., Millet, D. B., Bertram, T. H., Stanier, C. O., and Stone, E. A.: $PM_{2.5}$ chemistry, organosulfates, and secondary organic aerosol during the 2017 Lake Michigan Ozone Study, Atmos. Environ., 244, 117939, https://doi.org/10.1016/j.atmosenv.2020.117939, 2021.

Hyvärinen, A.-P., Raatikainen, T., Laaksonen, A., Viisanen, Y., and Lihavainen, H.: Surface tensions and densities of H2SO4 + NH3 + water solutions, Geophys. Res. Lett., 32, https://doi.org/10.1029/2005GL023268, 2005.

Intergovernmental Panel on Climate: C. Climate Change 2021 – The Physical Science Basis: Working Group I Contribution to the Sixth Assessment Report of the Intergovernmental Panel on Climate Change, Cambridge University Press, https://doi.org/10.1017/9781009157896, 2023.

Jeong, R., Lilek, J., Zuend, A., Xu, R., Chan, M. N., Kim, D., Moon, H. G., and Song, M.: Viscosity and physical state of sucrose mixed with ammonium sulfate droplets, Atmos. Chem. Phys., 22, 8805–8817, https://doi.org/10.5194/acp-22-8805-2022, 2022.

Joos, P. and Rillaerts, E.: Theory on the determination of the dynamic surface tension with the drop volume and maximum bubble pressure methods, J. Colloid Interf. Sci., 79, 96–100, https://doi.org/10.1016/0021-9797(81)90051-5, 1981.

Kampf, C. J., Waxman, E. M., Slowik, J. G., Dommen, J., Pfaffenberger, L., Praplan, A. P., Prévôt, A. S. H., Baltensperger, U., Hoffmann, T., and Volkamer, R.: Effective Henry's Law Partitioning and the Salting Constant of Glyoxal in Aerosols Containing Sulfate, Environ. Sci. Technol., 47, 4236–4244, https://doi.org/10.1021/es400083d, 2013.

Kanakidou, M., Seinfeld, J. H., Pandis, S. N., Barnes, I., Dentener, F. J., Facchini, M. C., Van Dingenen, R., Ervens, B., Nenes, A., Nielsen, C. J., Swietlicki, E., Putaud, J. P., Balkanski, Y., Fuzzi, S., Horth, J., Moortgat, G. K., Winterhalter, R., Myhre, C. E. L., Tsigaridis, K., Vignati, E., Stephanou, E. G., and Wilson, J.: Organic aerosol and global climate modelling: a review, Atmos. Chem. Phys., 5, 1053–1123, https://doi.org/10.5194/acp-5-1053-2005, 2005.

Kang, B., Tang, H., Zhao, Z., and Song, S.: Hofmeister Series: Insights of Ion Specificity from Amphiphilic Assembly and Interface Property, ACS Omega, 5, 6229–6239, https://doi.org/10.1021/acsomega.0c00237, 2020.

Kleinheins, J., Shardt, N., Lohmann, U., and Marcolli, C.: The surface tension and cloud condensation nuclei (CCN) activation of sea spray aerosol particles, Atmos. Chem. Phys., 25, 881–903, https://doi.org/10.5194/acp-25-881-2025, 2025.

Köhler, H.: The nucleus in and the growth of hygroscopic droplets, Transactions of the Faraday Society, 32, 1152–1161, https://doi.org/10.1039/TF9363201152, 1936.

Kreidenweis, S. M. and Asa-Awuku, A.: 5.13 - Aerosol Hygroscopicity: Particle Water Content and Its Role in Atmospheric Processes, in: Treatise on Geochemistry, 2nd edn., edited by: Holland, H. D. and Turekian, K. K., 331–361, Elsevier, https://doi.org/10.1016/B978-0-08-095975-7.00418-6, 2014.

Lance, S., Nenes, A., Medina, J., and Smith, J. N.: Mapping the Operation of the DMT Continuous Flow CCN Counter, Aerosol Sci. Technol., 40, 242–254, https://doi.org/10.1080/02786820500543290, 2006.

Laskina, O., Morris, H. S., Grandquist, J. R., Qin, Z., Stone, E. A., Tivanski, A. V., and Grassian, V. H.: Size Matters in the Water Uptake and Hygroscopic Growth of Atmospherically Relevant Multicomponent Aerosol Particles, J. Phys. Chem. A, 119, 4489–4497, https://doi.org/10.1021/jp510268p, 2015.

Leaist, D. G. and Hao, L.: Binary mutual diffusion coefficients of aqueous ammonium and potassium sulfates at 25 °C, Journal of Solution Chemistry, 21, 345–350, https://doi.org/10.1007/BF00647857, 1992.

Lin, Y.-H., Zhang, Z., Docherty, K. S., Zhang, H., Budisulistiorini, S. H., Rubitschun, C. L., Shaw, S. L., Knipping, E. M., Edgerton, E. S., Kleindienst, T. E., Gold, A., and Surratt, J. D.: Isoprene Epoxydiols as Precursors to Secondary Organic Aerosol Formation: Acid-Catalyzed Reactive Uptake Studies with Authentic Compounds, Environ. Sci. Technol., 46, 250–258, https://doi.org/10.1021/es202554c, 2012.

Malek, K., Gohil, K., Olonimoyo, E. A., Ferdousi-Rokib, N., Huang, Q., Pitta, K. R., Nandy, L., Voss, K. A., Raymond, T. M., Dutcher, D. D., Freedman, M. A., and Asa-Awuku, A.: Liquid–Liquid Phase Separation Can Drive Aerosol Droplet Growth in Supersaturated Regimes, ACS Environmental Au, 3, 348–360, https://doi.org/10.1021/acsenvironau.3c00015, 2023.

Mikhailov, E. F. and Vlasenko, S. S.: High-humidity tandem differential mobility analyzer for accurate determination of aerosol hygroscopic growth, microstructure, and activity coefficients over a wide range of relative humidity, Atmos. Meas. Tech., 13, 2035–2056, https://doi.org/10.5194/amt-13-2035-2020, 2020.

Mikhailov, E. F., Vlasenko, S. S., and Kiselev, A. A.: Water activity and surface tension of aqueous ammonium sulfate and D-glucose aerosol nanoparticles, Atmos. Chem. Phys., 24, 2971–2984, https://doi.org/10.5194/acp-24-2971-2024, 2024.

Moore, R. H., Nenes, A., and Medina, J.: Scanning Mobility CCN Analysis – A Method for Fast Measurements of Size-Resolved CCN Distributions and Activation Kinetics, Aerosol Sci. Technol., 44, 861–871, https://doi.org/10.1080/02786826.2010.498715, 2010.

Murphy, D. M., Thomson, D. S., and Mahoney, M. J.: In Situ Measurements of Organics, Meteoritic Material, Mercury, and Other Elements in Aerosols at 5 to 19 Kilometers, Science, 282, 1664–1669, https://doi.org/10.1126/science.282.5394.1664, 1998.

O'Meara, S., Topping, D. O., and McFiggans, G.: The rate of equilibration of viscous aerosol particles, Atmos. Chem. Phys., 16, 5299–5313, https://doi.org/10.5194/acp-16-5299-2016, 2016.

Ott, E.-J. E., Tackman, E. C., and Freedman, M. A.: Effects of Sucrose on Phase Transitions of Organic/Inorganic Aerosols, ACS Earth and Space Chemistry, 4, 591–601, https://doi.org/10.1021/acsearthspacechem.0c00006, 2020.

Padró, L. T., Tkacik, D., Lathem, T., Hennigan, C. J., Sullivan, A. P., Weber, R. J., Huey, L. G., and Nenes, A.: Investigation of cloud condensation nuclei properties and droplet growth kinetics of the water-soluble aerosol fraction in Mexico City, J. Geophys. Res.-Atmos., 115, https://doi.org/10.1029/2009JD013195, 2010.

Paramonov, M., Kerminen, V.-M., Gysel, M., Aalto, P. P., Andreae, M. O., Asmi, E., Baltensperger, U., Bougiatioti, A., Brus, D., Frank, G. P., Good, N., Gunthe, S. S., Hao, L., Irwin, M., Jaati- nen, A., Jurányi, Z., King, S. M., Kortelainen, A., Kristensson, A., Lihavainen, H., Kulmala, M., Lohmann, U., Martin, S. T., McFiggans, G., Mihalopoulos, N., Nenes, A., O'Dowd, C. D., Ovadnevaite, J., Petäjä, T., Pöschl, U., Roberts, G. C., Rose, D., Svenningsson, B., Swietlicki, E., Weingartner, E., Whitehead, J., Wiedensohler, A., Wittbom, C., and Sierau, B.: A synthesis of cloud condensation nuclei counter (CCNC) measurements within the EUCAARI network, Atmos. Chem. Phys., 15, 12211–12229, https://doi.org/10.5194/acp-15-12211-2015, 2015.

Paulot, F., Crounse, J. D., Kjaergaard, H. G., Kürten, A., St. Clair, J. M., Seinfeld, J. H., and Wennberg, P. O.: Unexpected Epoxide Formation in the Gas-Phase Photooxidation of Isoprene, Science, 325, 730–733, https://doi.org/10.1126/science.1172910, 2009.

Peng, C., Razafindrambinina, P. N., Malek, K. A., Chen, L., Wang, W., Huang, R.-J., Zhang, Y., Ding, X., Ge, M., Wang, X., Asa-Awuku, A. A., and Tang, M.: Interactions of organosulfates with water vapor under sub- and supersaturated conditions, Atmos. Chem. Phys., 21, 7135–7148, https://doi.org/10.5194/acp-21-7135-2021, 2021.

Petters, M. D. and Kreidenweis, S. M.: A single parameter representation of hygroscopic growth and cloud condensation nucleus activity, Atmos. Chem. Phys., 7, 1961–1971, https://doi.org/10.5194/acp-7-1961-2007, 2007.

Pratt, K. A. and Prather, K. A.: Aircraft measurements of vertical profiles of aerosol mixing states, J. Geophys. Res.-Atmos., 115, https://doi.org/10.1029/2009JD013150, 2010.

Prisle, N. L.: A predictive thermodynamic framework of cloud droplet activation for chemically unresolved aerosol mixtures, including surface tension, non-ideality, and bulk–surface partitioning, Atmos. Chem. Phys., 21, 16387–16411, https://doi.org/10.5194/acp-21-16387-2021, 2021.

Prisle, N. L., Engelhart, G. J., Bilde, M., and Donahue, N. M.: Humidity influence on gas-particle phase partitioning of á-pinene + O3 secondary organic aerosol, Geophys. Res. Lett., 37, https://doi.org/10.1029/2009GL041402, 2010.

Pruppacher, H. R. and Klett, J. D.: Microphysics of Clouds and Precipitation, Springer, 954 pp., https://books.google.com/books?id=Nk40jwEACAAJ (last access: 11 February 2025), 1997.

Reid, J. P., Bertram, A. K., Topping, D. O., Laskin, A., Martin, S. T., Petters, M. D., Pope, F. D., and Rovelli, G.: The viscosity of atmospherically relevant organic particles, Nat. Commun., 9, 956, https://doi.org/10.1038/s41467-018-03027-z, 2018.

Renbaum-Wolff, L., Grayson, J. W., Bateman, A. P., Kuwata, M., Sellier, M., Murray, B. J., Shilling, J. E., Martin, S. T., and Bertram, A. K.: Viscosity of α-pinene secondary organic material and implications for particle growth and reactivity, P. Natl. Acad. Sci. USA, 110, 8014–8019, https://doi.org/10.1073/pnas.1219548110, 2013.

Riemer, N., Ault, A. P., West, M., Craig, R. L., and Curtis, J. H.: Aerosol Mixing State: Measurements, Modeling, and Impacts, Rev. Geophys., 57, 187–249, https://doi.org/10.1029/2018RG000615, 2019.

Riipinen, I., Pierce, J. R., Yli-Juuti, T., Nieminen, T., Häkkinen, S., Ehn, M., Junninen, H., Lehtipalo, K., Petäjä, T., Slowik, J., Chang, R., Shantz, N. C., Abbatt, J., Leaitch, W. R., Kerminen, V.-M., Worsnop, D. R., Pandis, S. N., Donahue, N. M., and Kulmala, M.: Organic condensation: a vital link connecting aerosol formation to cloud condensation nu-

clei (CCN) concentrations, Atmos. Chem. Phys., 11, 3865–3878, https://doi.org/10.5194/acp-11-3865-2011, 2011.

Riva, M., Chen, Y., Zhang, Y., et al.: Increasing Isoprene Epoxydiol-to-Inorganic Sulfate Aerosol Ratio Results in Extensive Conversion of Inorganic Sulfate to Organosulfur Forms: Implications for Aerosol Physicochemical Properties, Environ. Sci. Technol., 53, 8682–8694, https://doi.org/10.1021/acs.est.9b01019, 2019.

Roberts, G. C. and Nenes, A.: A Continuous-Flow Streamwise Thermal-Gradient CCN Chamber for Atmospheric Measurements, Aerosol Sci. Technol., 39, 206–221, https://doi.org/10.1080/027868290913988, 2005.

Rose, D., Gunthe, S. S., Mikhailov, E., Frank, G. P., Dusek, U., Andreae, M. O., and Pöschl, U.: Calibration and measurement uncertainties of a continuous-flow cloud condensation nuclei counter (DMT-CCNC): CCN activation of ammonium sulfate and sodium chloride aerosol particles in theory and experiment, Atmos. Chem. Phys., 8, 1153–1179, https://doi.org/10.5194/acp-8-1153-2008, 2008.

Ross, S.: The Change of Surface Tension with Time. I. Theories of Diffusion to the Surface, J. Am. Chem. Soc., 67, 990–994, https://doi.org/10.1021/ja01222a031, 1945.

Ruehl, C. R., Chuang, P. Y., Nenes, A., Cappa, C. D., Kolesar, K. R., and Goldstein, A. H.: Strong evidence of surface tension reduction in microscopic aqueous droplets, Geophys. Res. Lett., 39, https://doi.org/10.1029/2012GL053706, 2012.

Ruehl, C. R., Davies, J. F., and Wilson, K. R.: An interfacial mechanism for cloud droplet formation on organic aerosols, Science, 351, 1447–1450, https://doi.org/10.1126/science.aad4889, 2016.

Saukko, E., Lambe, A. T., Massoli, P., Koop, T., Wright, J. P., Croasdale, D. R., Pedernera, D. A., Onasch, T. B., Laaksonen, A., Davidovits, P., Worsnop, D. R., and Virtanen, A.: Humidity-dependent phase state of SOA particles from biogenic and anthropogenic precursors, Atmos. Chem. Phys., 12, 7517–7529, https://doi.org/10.5194/acp-12-7517-2012, 2012.

Saxena, P., Hildemann, L. M., McMurry, P. H., and Seinfeld, J. H.: Organics alter hygroscopic behavior of atmospheric particles, J. Geophys. Res.-Atmos., 100, 18755–18770, https://doi.org/10.1029/95JD01835, 1995.

Schmedding, R. and Zuend, A.: The role of interfacial tension in the size-dependent phase separation of atmospheric aerosol particles, Atmos. Chem. Phys., 25, 327–346, https://doi.org/10.5194/acp-25-327-2025, 2025.

Seinfeld, J. and Pandis, S.: Atmospheric Chemistry and Physics: From Air Pollution to Climate Change, John Wiley & Sons, Inc., Hoboken, NJ, ISBN: 978-0-471-72018-8, 1998.

Seinfeld, J. H.: TROPOSPHERIC CHEMISTRY AND COMPOSITION | Aerosols/Particles, in: Encyclopedia of Atmospheric Sciences, edited by: Holton, J. R., 2349–2354, Academic Press, https://doi.org/10.1016/B0-12-227090-8/00438-3, 2003.

Sheldon, C. S., Choczynski, J. M., Morton, K., Palacios Diaz, T., Davis, R. D., and Davies, J. F.: Exploring the hygroscopicity, water diffusivity, and viscosity of organic–inorganic aerosols – a case study on internally-mixed citric acid and ammonium sulfate particles, Environmental Science: Atmospheres, 3, 24–34, https://doi.org/10.1039/D2EA00116K, 2023.

Shiraiwa, M. and Seinfeld, J. H.: Equilibrium timescale of atmospheric secondary organic aerosol partitioning, Geophys. Res. Lett., 39, https://doi.org/10.1029/2012GL054008, 2012.

Shiraiwa, M., Li, Y., Tsimpidi, A. P., Karydis, V. A., Berkemeier, T., Pandis, S. N., Lelieveld, J., Koop, T., and Pöschl, U.: Global distribution of particle phase state in atmospheric secondary organic aerosols, Nat. Commun., 8, 15002, https://doi.org/10.1038/ncomms15002, 2017.

Sindelarova, K., Granier, C., Bouarar, I., Guenther, A., Tilmes, S., Stavrakou, T., Müller, J.-F., Kuhn, U., Stefani, P., and Knorr, W.: Global data set of biogenic VOC emissions calculated by the MEGAN model over the last 30 years, Atmos. Chem. Phys., 14, 9317–9341, https://doi.org/10.5194/acp-14-9317-2014, 2014.

Song, M., Marcolli, C., Krieger, U. K., Lienhard, D. M., and Peter, T.: Morphologies of mixed organic/inorganic/aqueous aerosol droplets, Faraday Discuss., 165, 289–316, https://doi.org/10.1039/C3FD00049D, 2013.

Spelt, J.: Applied Surface Thermodynamics, Crc Press, edited by: Spelt, J. K. and Neumann, A. W., Marcel Dekker, Inc., New York, NY, https://doi.org/10.1201/9780585157719, 1996.

Srivastava, D., Vu, T. V., Tong, S., Shi, Z., and Harrison, R. M.: Formation of secondary organic aerosols from anthropogenic precursors in laboratory studies, npj Climate and Atmospheric Science, 5, 22, https://doi.org/10.1038/s41612-022-00238-6, 2022.

Sullivan, R. C., Moore, M. J. K., Petters, M. D., Kreidenweis, S. M., Roberts, G. C., and Prather, K. A.: Effect of chemical mixing state on the hygroscopicity and cloud nucleation properties of calcium mineral dust particles, Atmos. Chem. Phys., 9, 3303–3316, https://doi.org/10.5194/acp-9-3303-2009, 2009.

Surratt, J. D., Chan, A. W. H., Eddingsaas, N. C., Chan, M., Loza, C. L., Kwan, A. J., Hersey, S. P., Flagan, R. C., Wennberg, P. O., and Seinfeld, J. H.: Reactive intermediates revealed in secondary organic aerosol formation from isoprene, P. Natl. Acad. Sci. USA, 107, 6640–6645, https://doi.org/10.1073/pnas.0911114107, 2010.

Tandon, A., Rothfuss, N. E., and Petters, M. D.: The effect of hydrophobic glassy organic material on the cloud condensation nuclei activity of particles with different morphologies, Atmos. Chem. Phys., 19, 3325–3339, https://doi.org/10.5194/acp-19-3325-2019, 2019.

Toivola, M., Prisle, N. L., Elm, J., Waxman, E. M., Volkamer, R., and Kurtén, T.: Can COSMOTherm Predict a Salting in Effect?, J. Phys. Chem. A, 121, 6288–6295, https://doi.org/10.1021/acs.jpca.7b04847, 2017.

Topping, D.: An analytical solution to calculate bulk mole fractions for any number of components in aerosol droplets after considering partitioning to a surface layer, Geosci. Model Dev., 3, 635–642, https://doi.org/10.5194/gmd-3-635-2010, 2010.

Topping, D. O., McFiggans, G. B., Kiss, G., Varga, Z., Facchini, M. C., Decesari, S., and Mircea, M.: Surface tensions of multicomponent mixed inorganic/organic aqueous systems of atmospheric significance: measurements, model predictions and importance for cloud activation predictions, Atmos. Chem. Phys., 7, 2371–2398, https://doi.org/10.5194/acp-7-2371-2007, 2007.

Twomey, S.: The nuclei of natural cloud formation part II: The supersaturation in natural clouds and the variation of cloud droplet concentration, Geofisica pura e applicata, 43, 243–249, https://doi.org/10.1007/BF01993560, 1959.

Twomey, S.: Pollution and the planetary albedo, Atmos. Environ., 8, 1251–1256, https://doi.org/10.1016/0004-6981(74)90004-3, 1974.

Veghte, D. P., Altaf, M. B., and Freedman, M. A.: Size Dependence of the Structure of Organic Aerosol, J. Am. Chem. Soc., 135, 16046–16049, https://doi.org/10.1021/ja408903g, 2013.

Vepsäläinen, S., Calderón, S. M., and Prisle, N. L.: Comparison of six approaches to predicting droplet activation of surface active aerosol – Part 2: Strong surfactants, Atmos. Chem. Phys., 23, 15149–15164, https://doi.org/10.5194/acp-23-15149-2023, 2023.

Vignes, A.: Diffusion in Binary Solutions. Variation of Diffusion Coefficient with Composition, Industrial & Engineering Chemistry Fundamentals, 5, 189–199, https://doi.org/10.1021/i160018a007, 1966.

Virtanen, A., Joutsensaari, J., Koop, T., Kannosto, J., Yli-Pirilä, P., Leskinen, J., Mäkelä, J. M., Holopainen, J. K., Pöschl, U., Kulmala, M., Worsnop, D. R., and Laaksonen, A.: An amorphous solid state of biogenic secondary organic aerosol particles, Nature, 467, 824–827, https://doi.org/10.1038/nature09455, 2010.

Vitagliano, V. and Lyons, P. A.: Diffusion Coefficients for Aqueous Solutions of Sodium Chloride and Barium Chloride, J. Am. Chem. Soc., 78, 1549–1552, https://doi.org/10.1021/ja01589a011, 1956.

Vizenor, A. E. and Asa-Awuku, A. A.: Gas-phase kinetics modifies the CCN activity of a biogenic SOA, Phys. Chem. Chem. Phys., 20, 6591–6597, https://doi.org/10.1039/C8CP00075A, 2018.

Wallace, B. J., Price, C. L., Davies, J. F., and Preston, T. C.: Multicomponent diffusion in atmospheric aerosol particles, Environmental Science: Atmospheres, 1, 45–55, https://doi.org/10.1039/D0EA00008F, 2021.

Wang, M., Wu, P., Sengupta, S. S., Chadhary, B. I., Cogen, J. M., and Li, B.: Investigation of Water Diffusion in Low-Density Polyethylene by Attenuated Total Reflectance Fourier Transform Infrared Spectroscopy and Two-Dimensional Correlation Analysis, Industrial & Engineering Chemistry Research, 50, 6447–6454, https://doi.org/10.1021/ie102221a, 2011.

Werner, E. K., Hammond, M., and Bain, A.: Surface tension predictions during hygroscopic growth and cloud droplet activation using a simple kinetic surfactant partitioning model, Aerosol Sci. Technol., 59, 781–793, https://doi.org/10.1080/02786826.2025.2465705, 2025.

Wex, H., Stratmann, F., Topping, D., and McFiggans, G.: The Kelvin versus the Raoult Term in the Köhler Equation, J. Atmos. Sci., 65, 4004–4016, https://doi.org/10.1175/2008JAS2720.1, 2008.

Wiedensohler, A.: An approximation of the bipolar charge distribution for particles in the submicron size range, J. Aerosol Sci., 19, 387–389, 1988.

Wolf, M. J., Zhang, Y., Zhou, J., Surratt, J. D., Turpin, B. J., and Cziczo, D. J.: Enhanced Ice Nucleation of Simulated Sea Salt Particles with the Addition of Anthropogenic Per- and Polyfluoroalkyl Substances, ACS Earth and Space Chemistry, 5, 2074–2085, https://doi.org/10.1021/acsearthspacechem.1c00138, 2021.

Wu, L., Li, X., Kim, H., Geng, H., Godoi, R. H. M., Barbosa, C. G. G., Godoi, A. F. L., Yamamoto, C. I., de Souza, R. A. F., Pöhlker, C., Andreae, M. O., and Ro, C.-U.: Single-particle characterization of aerosols collected at a remote site in the Amazonian rainforest and an urban site in Manaus, Brazil, Atmos. Chem. Phys., 19, 1221–1240, https://doi.org/10.5194/acp-19-1221-2019, 2019.

Yang, F., Chen, H., Wang, X., Yang, X., Du, J., and Chen, J.: Single particle mass spectrometry of oxalic acid in ambient aerosols in Shanghai: Mixing state and formation mechanism, Atmos. Environ., 43, 3876–3882, https://doi.org/10.1016/j.atmosenv.2009.05.002, 2009.

Zhang, C., Lu, M., Ma, N., Yang, Y., Wang, Y., Größ, J., Fan, Z., Wang, M., and Wiedensohler, A.: Hygroscopicity of aerosol particles composed of surfactant SDS and its internal mixture with ammonium sulfate at relative humidities up to 99.9 %, Atmos. Environ., 298, 119625, https://doi.org/10.1016/j.atmosenv.2023.119625, 2023.

Zhang, Q., Jimenez, J. L., Canagaratna, M. R., Allan, J. D., Coe, H., Ulbrich, I., Alfarra, M. R., Takami, A., Middlebrook, A. M., Sun, Y. L., Dzepina, K., Dunlea, E., Docherty, K., DeCarlo, P. F., Salcedo, D., Onasch, T., Jayne, J. T., Miyoshi, T., Shimono, A., Hatakeyama, S., Takegawa, N., Kondo, Y., Schneider, J., Drewnick, F., Borrmann, S., Weimer, S., Demerjian, K., Williams, P., Bower, K., Bahreini, R., Cottrell, L., Griffin, R. J., Rautiainen, J., Sun, J. Y., Zhang, Y. M., and Worsnop, D. R.: Ubiquity and dominance of oxygenated species in organic aerosols in anthropogenically-influenced Northern Hemisphere midlatitudes, Geophys. Res. Lett., 34, https://doi.org/10.1029/2007GL029979, 2007.

Zhang, Y., Sanchez, M. S., Douet, C., Wang, Y., Bateman, A. P., Gong, Z., Kuwata, M., Renbaum-Wolff, L., Sato, B. B., Liu, P. F., Bertram, A. K., Geiger, F. M., and Martin, S. T.: Changing shapes and implied viscosities of suspended submicron particles, Atmos. Chem. Phys., 15, 7819–7829, https://doi.org/10.5194/acp-15-7819-2015, 2015.

Zhang, Y., Chen, Y., Lambe, A. T., Olson, N. E., Lei, Z., Craig, R. L., Zhang, Z., Gold, A., Onasch, T. B., Jayne, J. T., Worsnop, D. R., Gaston, C. J., Thornton, J. A., Vizuete, W., Ault, A. P., and Surratt, J. D.: Effect of the Aerosol-Phase State on Secondary Organic Aerosol Formation from the Reactive Uptake of Isoprene-Derived Epoxydiols (IEPOX), Environ. Sci. Technol. Lett., 5, 167–174, https://doi.org/10.1021/acs.estlett.8b00044, 2018.

Zhang, Y., Chen, Y., Lei, Z., Olson, N. E., Riva, M., Koss, A. R., Zhang, Z., Gold, A., Jayne, J. T., Worsnop, D. R., Onasch, T. B., Kroll, J. H., Turpin, B. J., Ault, A. P., and Surratt, J. D.: Joint Impacts of Acidity and Viscosity on the Formation of Secondary Organic Aerosol from Isoprene Epoxydiols (IEPOX) in Phase Separated Particles, ACS Earth and Space Chemistry, 3, 2646–2658, https://doi.org/10.1021/acsearthspacechem.9b00209, 2019a.

Zhang, Y., Nichman, L., Spencer, P., Jung, J. I., Lee, A., Heffernan, B. K., Gold, A., Zhang, Z., Chen, Y., Canagaratna, M. R., Jayne, J. T., Worsnop, D. R., Onasch, T. B., Surratt, J. D., Chandler, D., Davidovits, P., and Kolb, C. E.: The Cooling Rate- and Volatility-Dependent Glass-Forming Properties of Organic Aerosols Measured by Broadband Dielectric Spectroscopy, Environ. Sci. Technol., 53, 12366–12378, https://doi.org/10.1021/acs.est.9b03317, 2019b.

Zhu, J., Penner, J. E., Lin, G., Zhou, C., Xu, L., and Zhuang, B.: Mechanism of SOA formation determines magnitude of radiative effects, P. Natl. Acad. Sci. USA, 114, 12685–12690, https://doi.org/10.1073/pnas.1712273114, 2017.